

Supporting Information 1

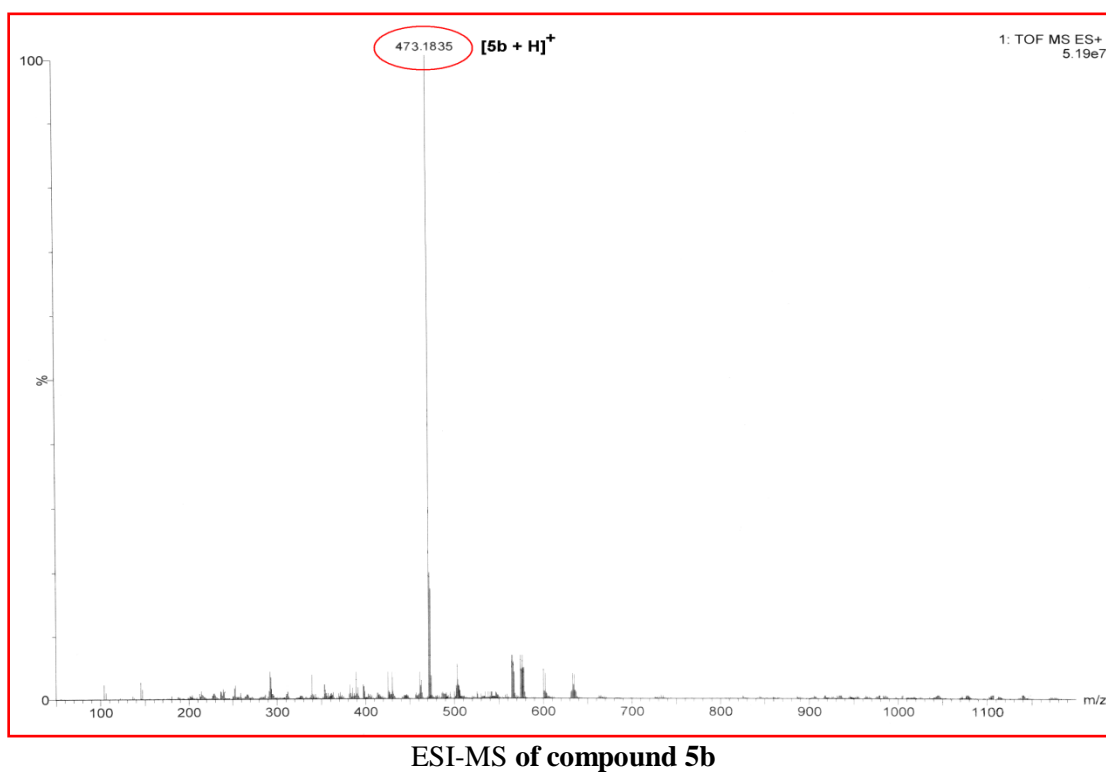
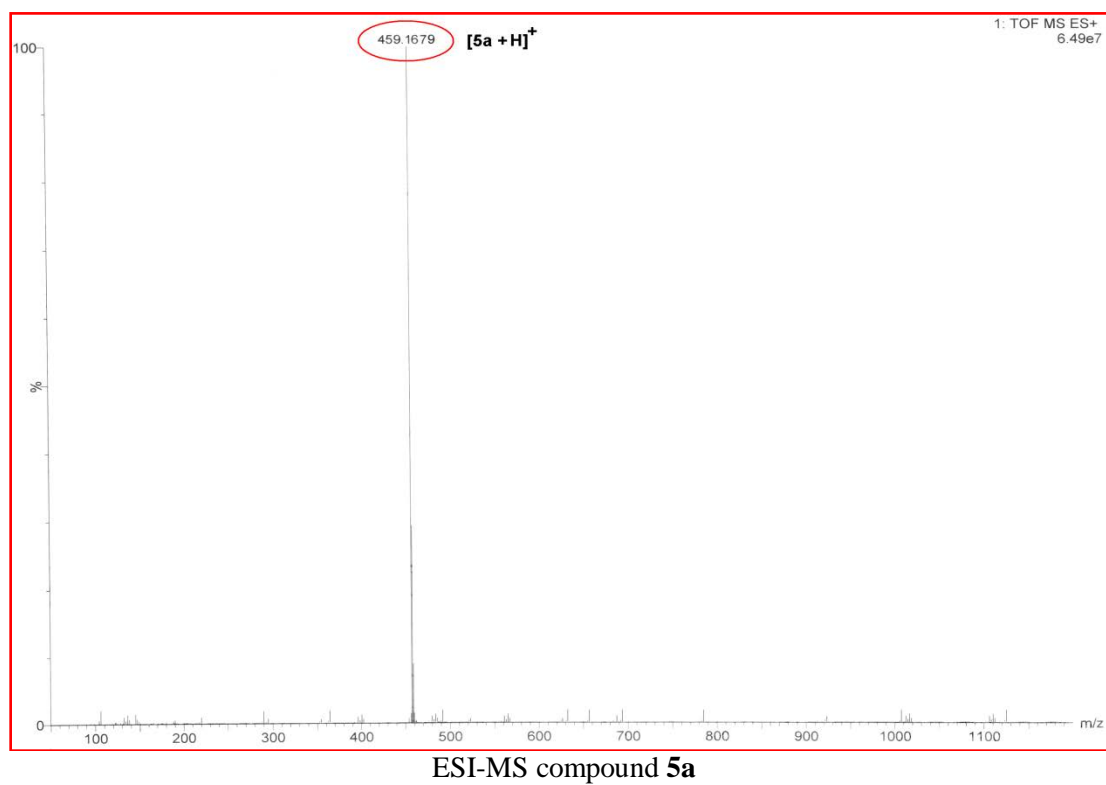
I₂ catalyzed access of spiro[indoline-3,4'-pyridine] appended amine dyad: New ON-OFF chemosensors for Cu²⁺ and imaging in living cells

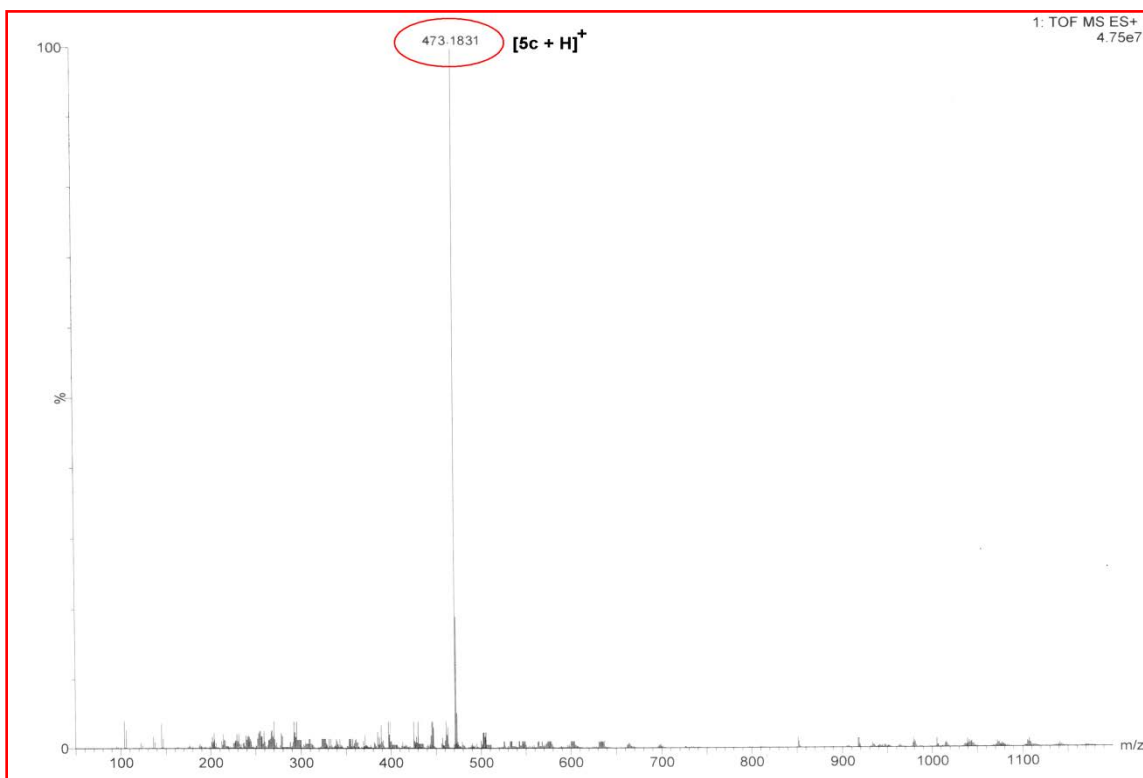
**Animesh Mondal^a, Barnali Naskar^a, Sanchita Goswami^a, Chandraday Prodhana^b, Keya Chaudhuri^b
and Chhanda Mukhopadhyay^{a*}**

*E-mail: cmukhop@yahoo.co.in

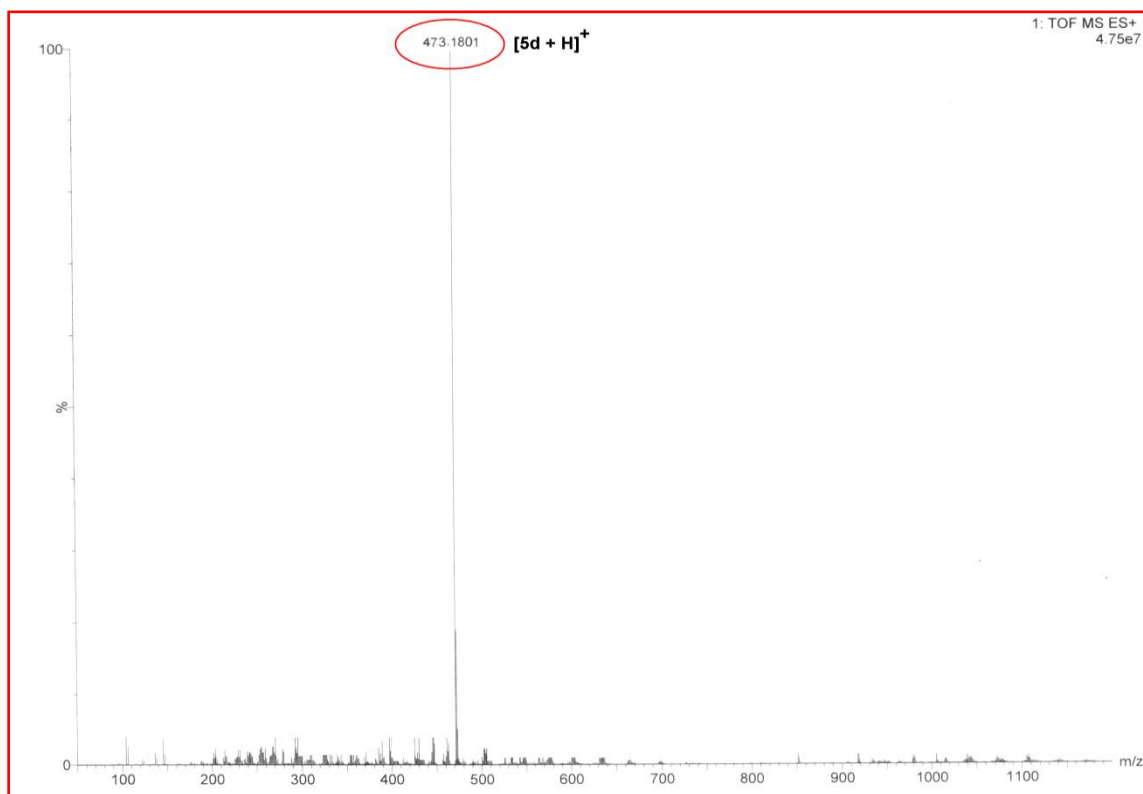
Table of Contents	Pages
Figure S1. ESI-MS spectra of compound 5a-5f, 5h-5l and in copper complexes	... 03-13
Photophysical Characterization	
Figure S2-12. Absorption spectra of compounds 5a-5f and 5h-5l upon titration with Cu^{2+}	... 14-19
Figure S13-17. Fluorescence Quenching Efficiency (FQE) of compounds 5d, 5f, 5h, 5j and 5k	... 20-22
Figure S18-28. Job's plot for determination of stoichiometry of Cu^{2+} : in solution of complexes 5a-5f and 5h-5l	... 23-28
Figure S29-33. Benesi-Hildebrand plot of fluorescence titration curves of 5d, 5f, 5h, 5j and 5k with Cu^{2+}	... 29-31
Figure S34-38. The limit of detection (LOD) of compounds 5d, 5f, 5h, 5j and 5k for Cu^{2+} as a function of $[\text{Cu}^{2+}]$... 32-34
Figure S39-43. Fluorescence emission spectra of chemosensor (5d, 5f, 5h, 5j and 5k) in the presence of Cu^{2+} ion followed by addition of EDTA	... 35-37
Figure S44-48. Emission intensity of compounds 5d, 5f, 5h, 5j and 5k in absence and in presence of Cu^{2+} at different pH values in aqueous DMSO solution	... 38-40

Figure S1. ESI-MS spectra of compound 5a–5f, 5h–5l and in copper complexes:

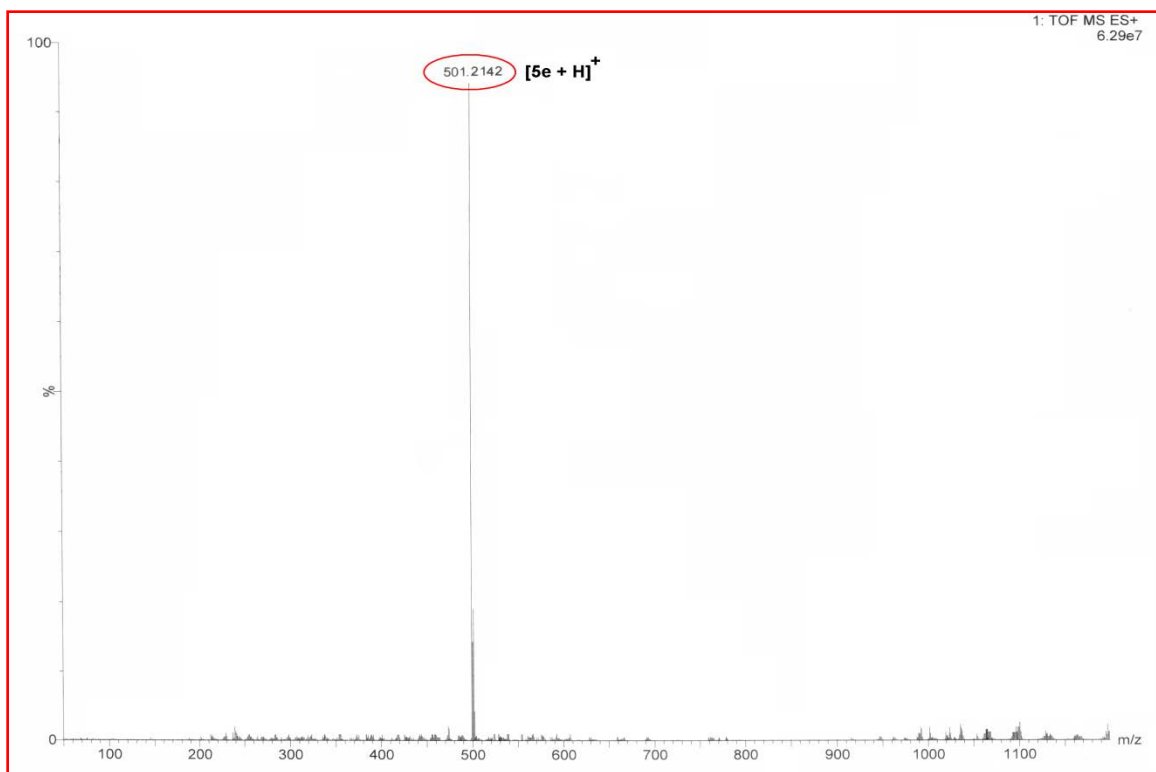




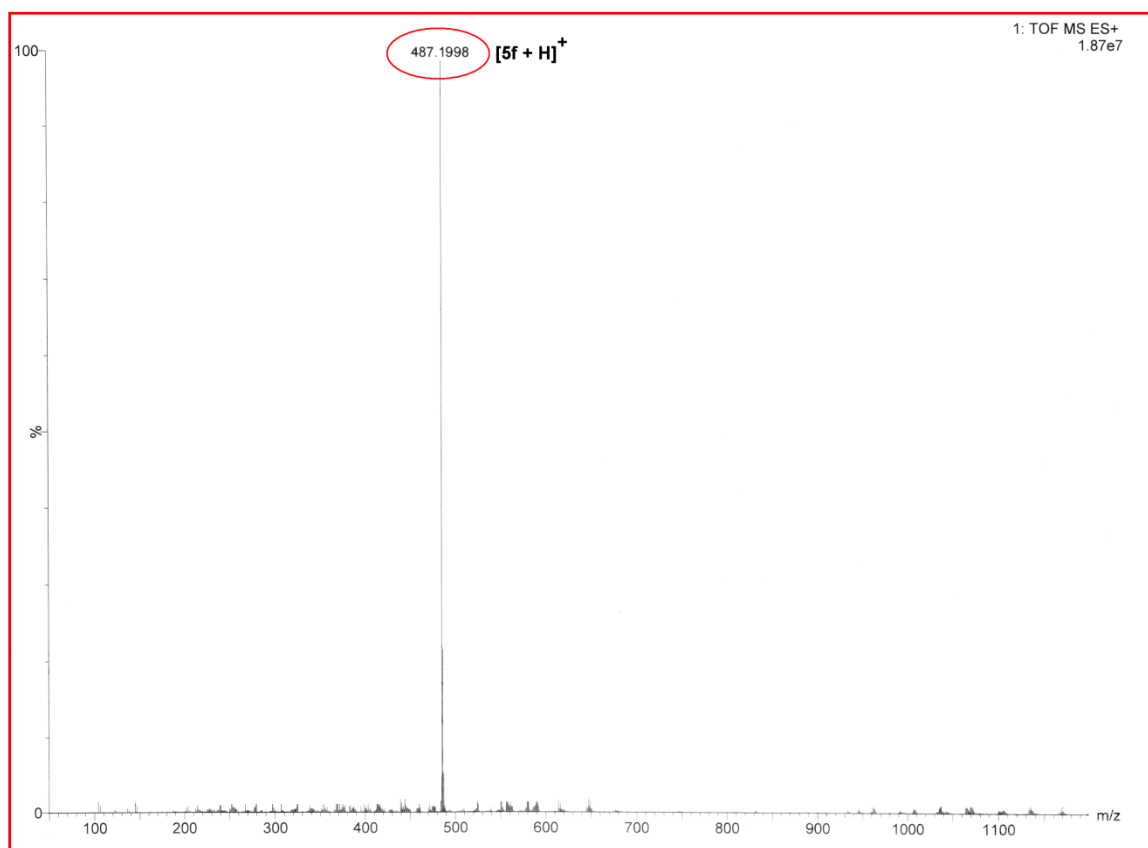
ESI-MS of compound **5c**



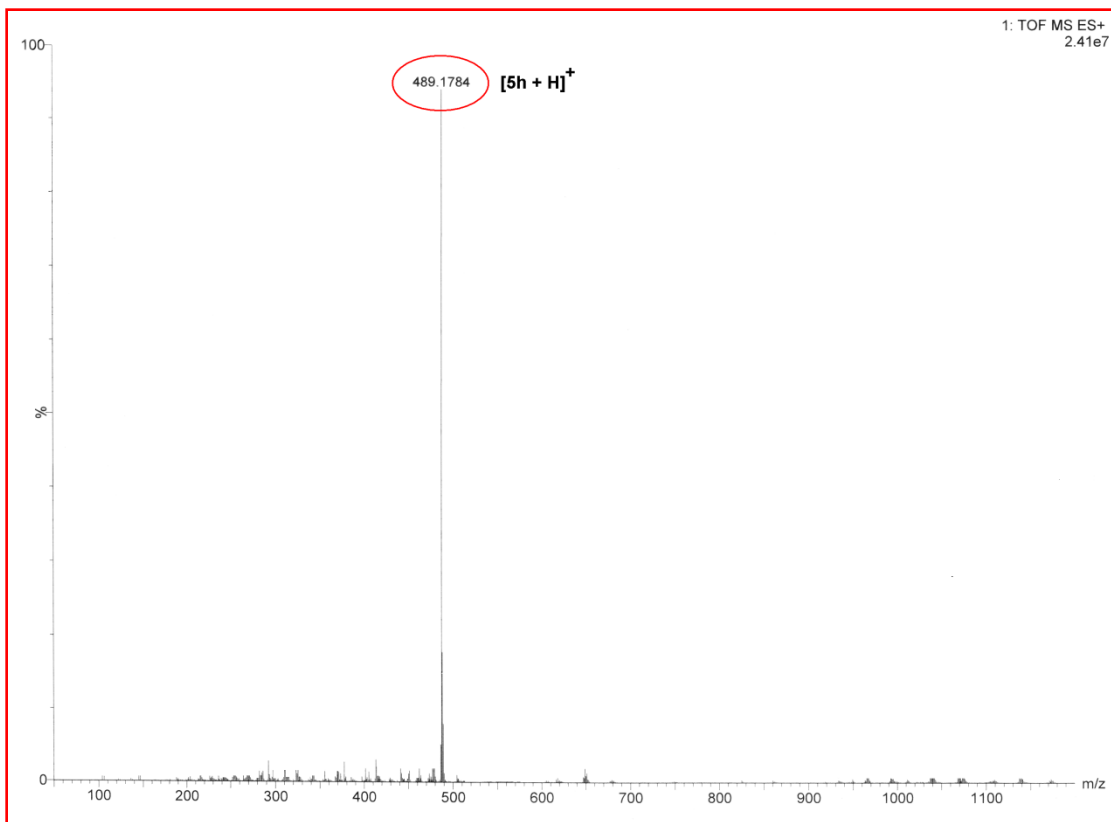
ESI-MS of compound **5d**



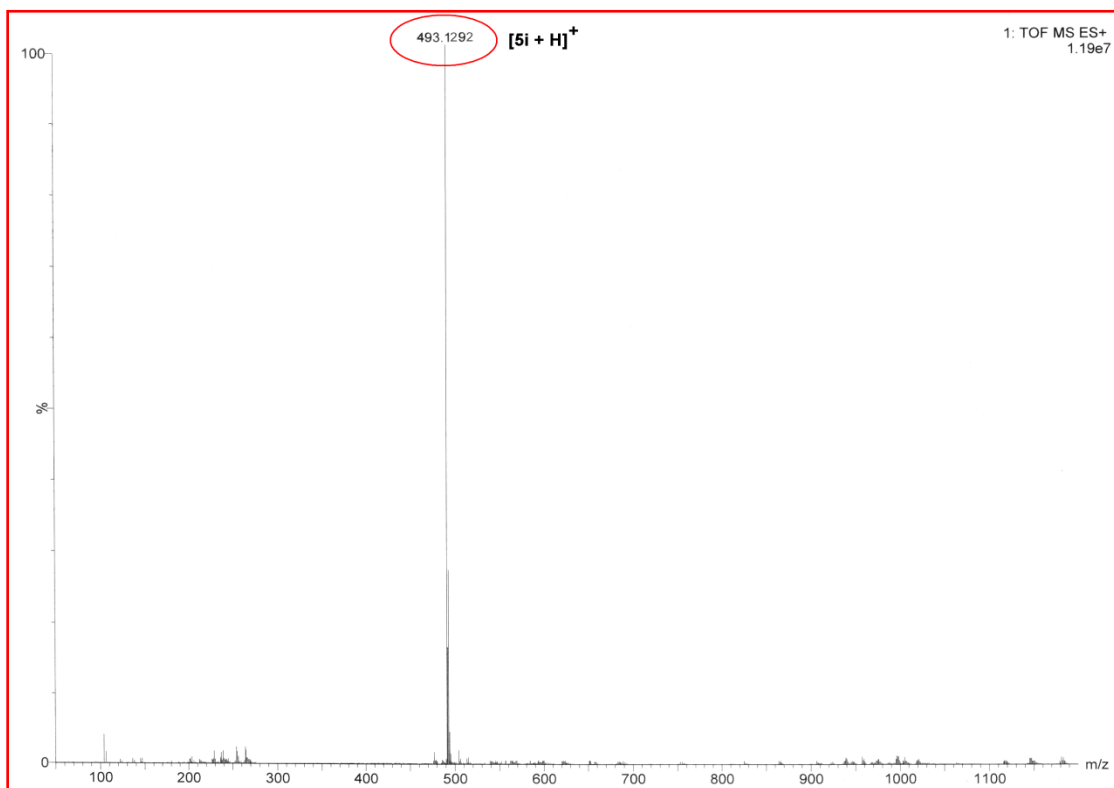
ESI-MS of compound **5e**



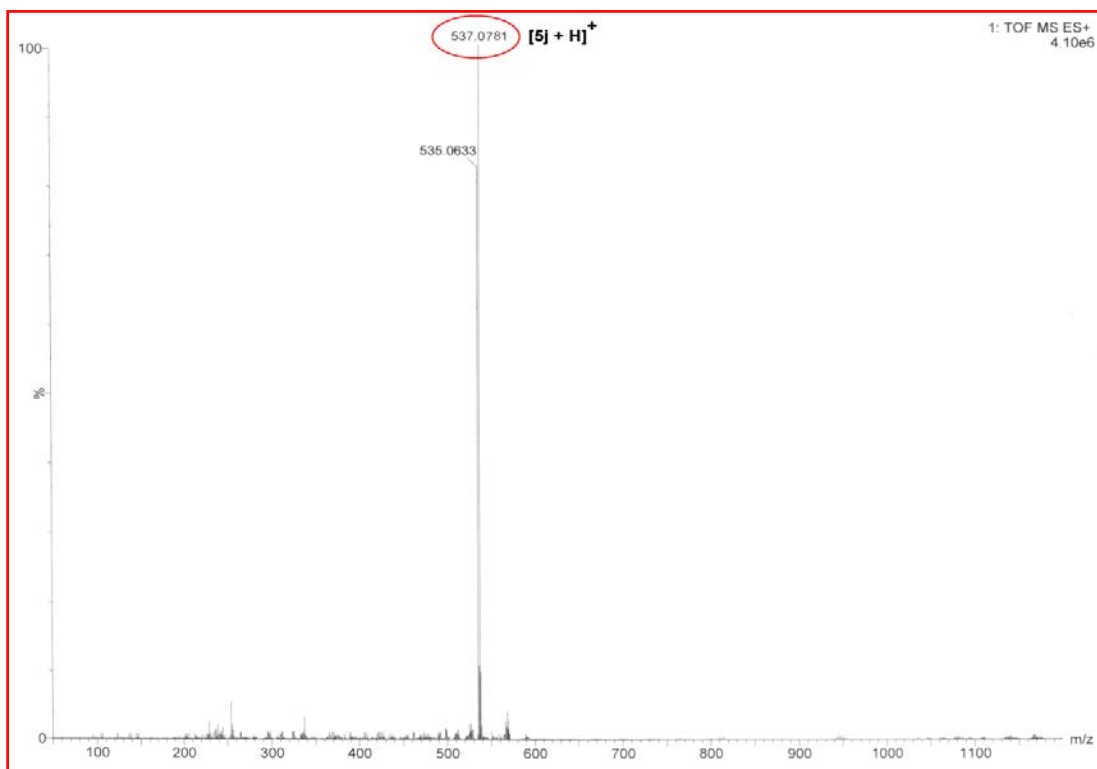
ESI-MS of compound **5f**



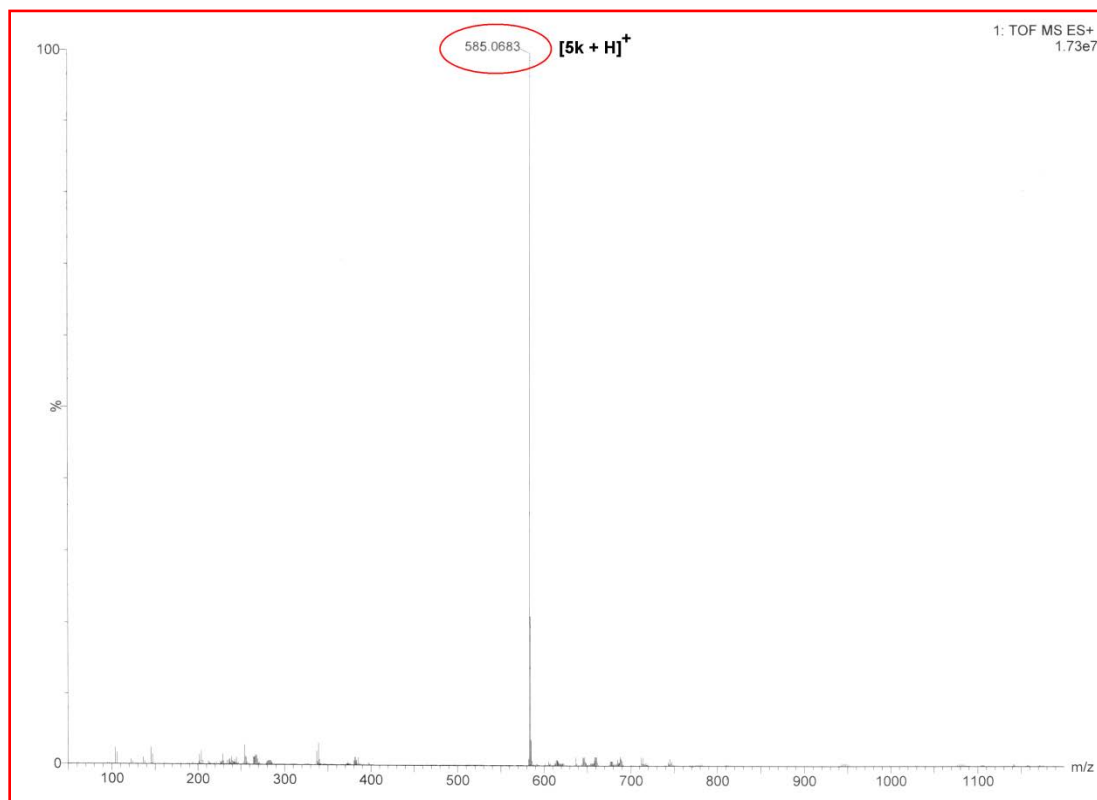
ESI-MS of compound **5h**



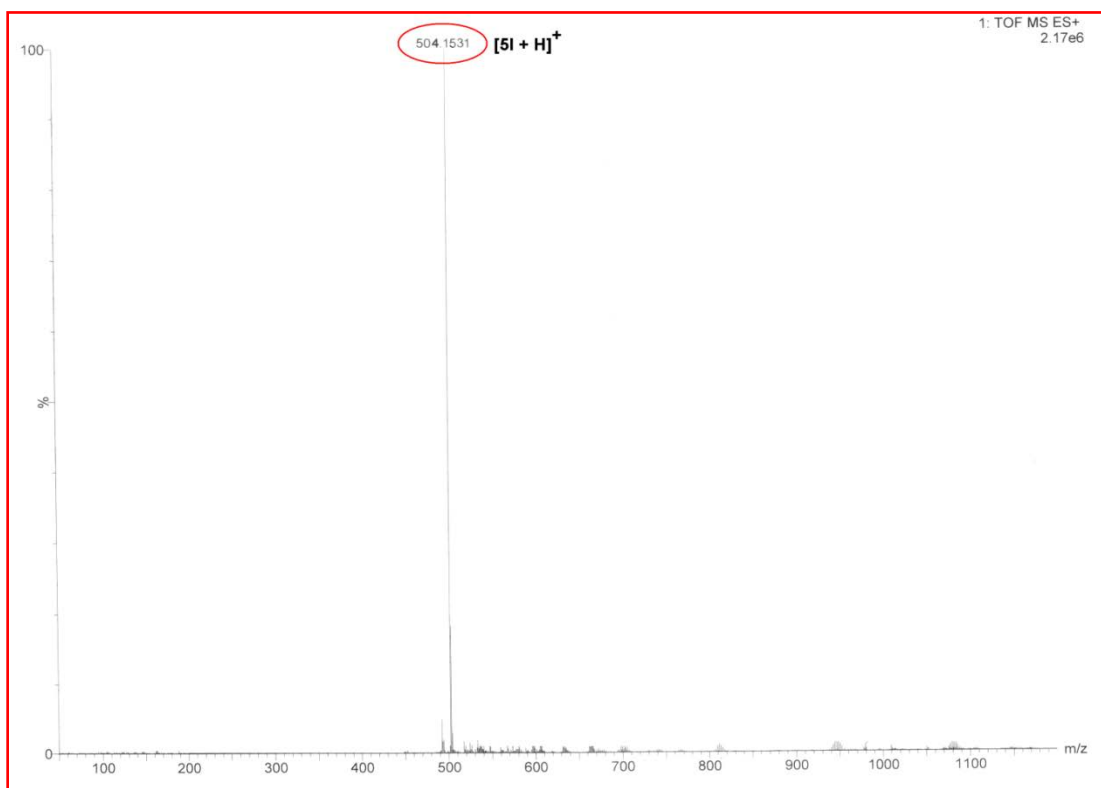
ESI-MS of compound **5i**



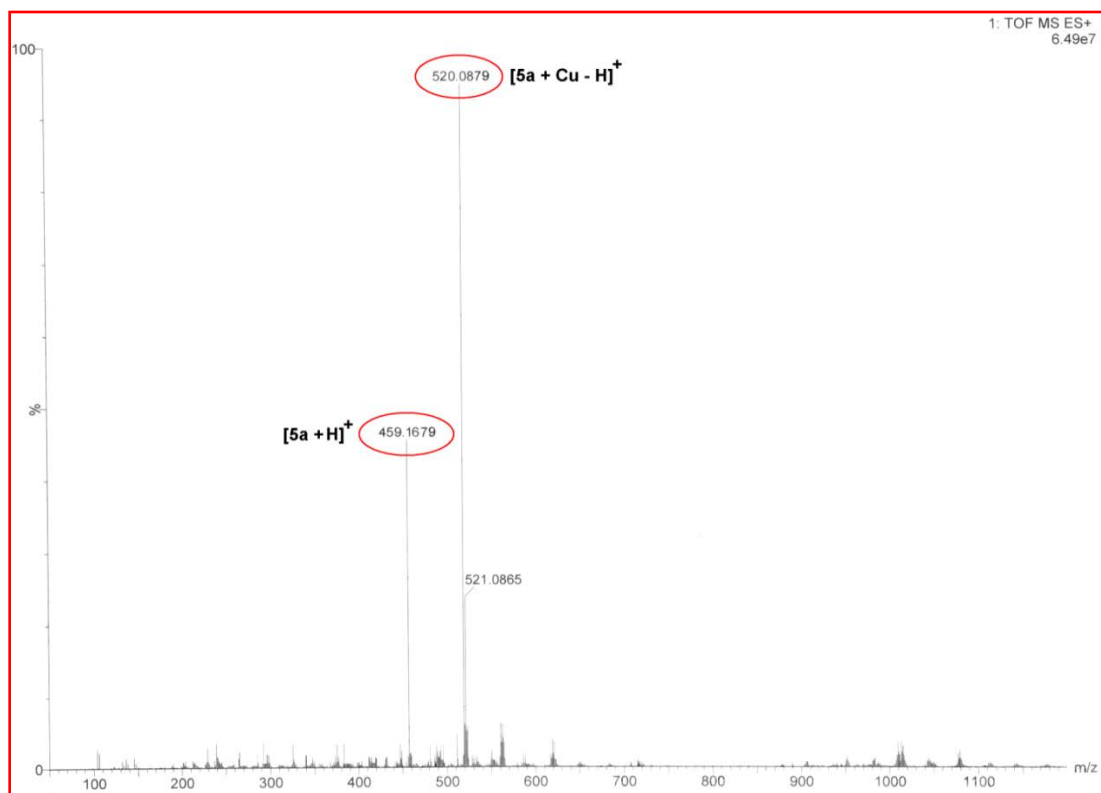
ESI-MS of compound **5j**



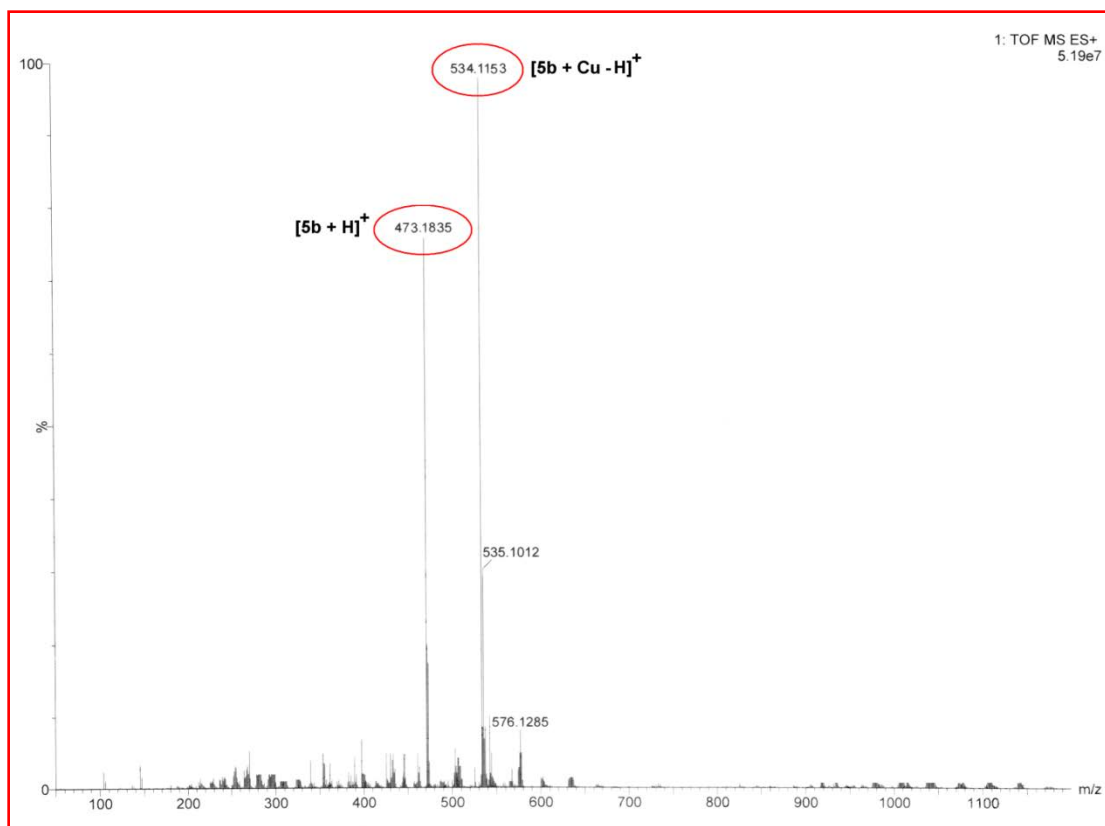
ESI-MS of compound **5k**



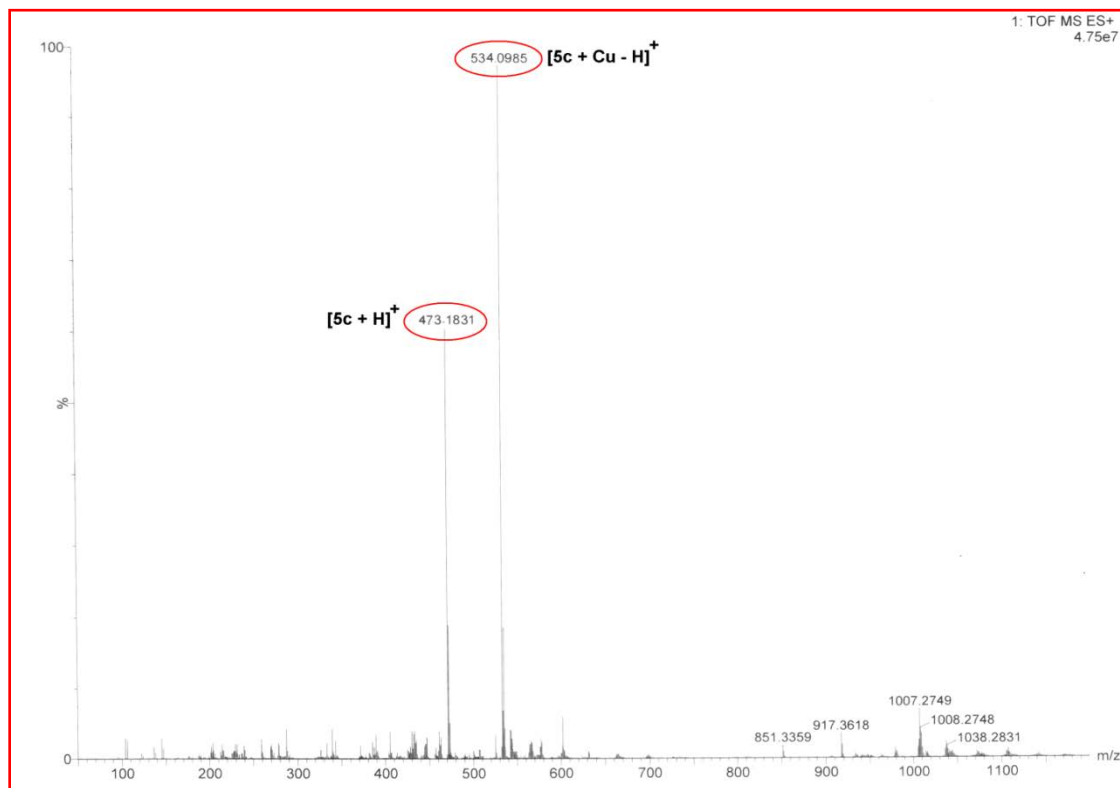
ESI-MS of compound **5I**



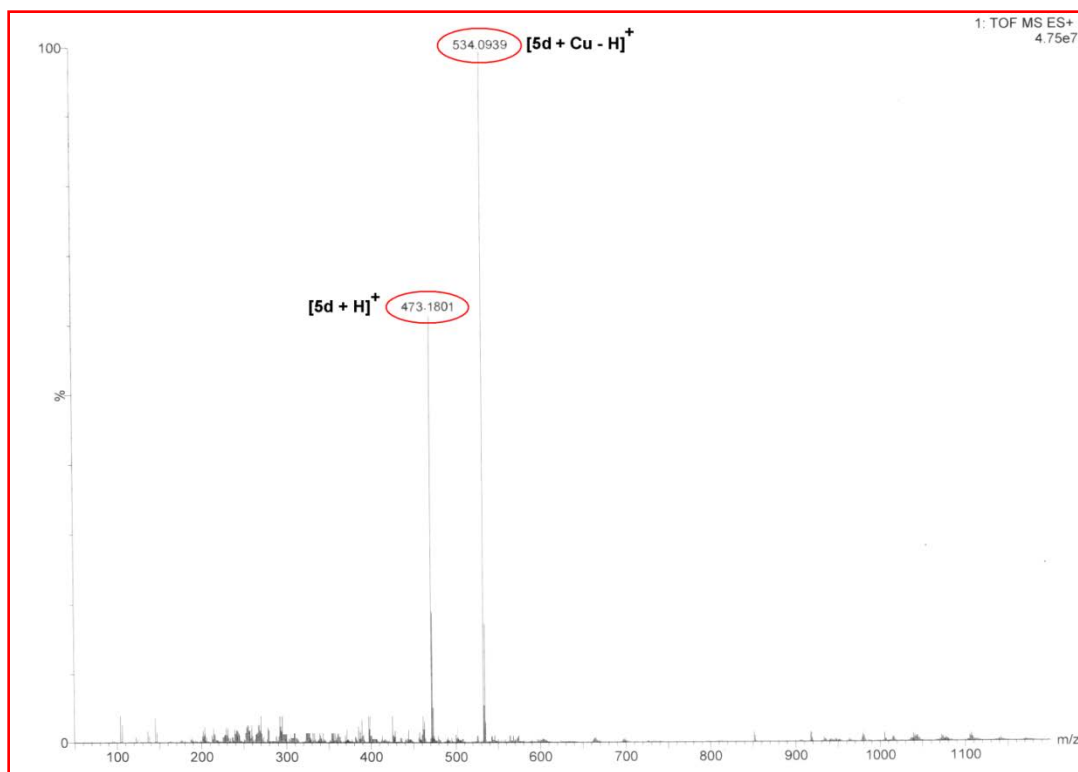
ESI-MS of compound **5a+Cu**



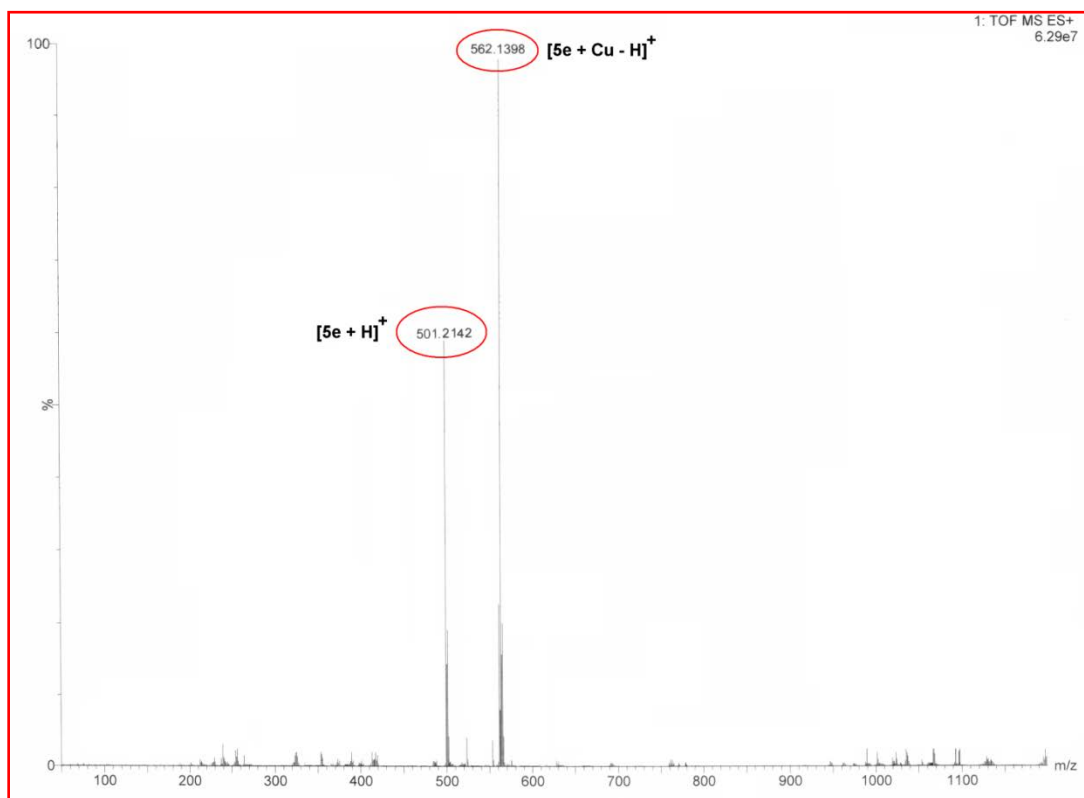
ESI-MS of compound **5b+Cu**



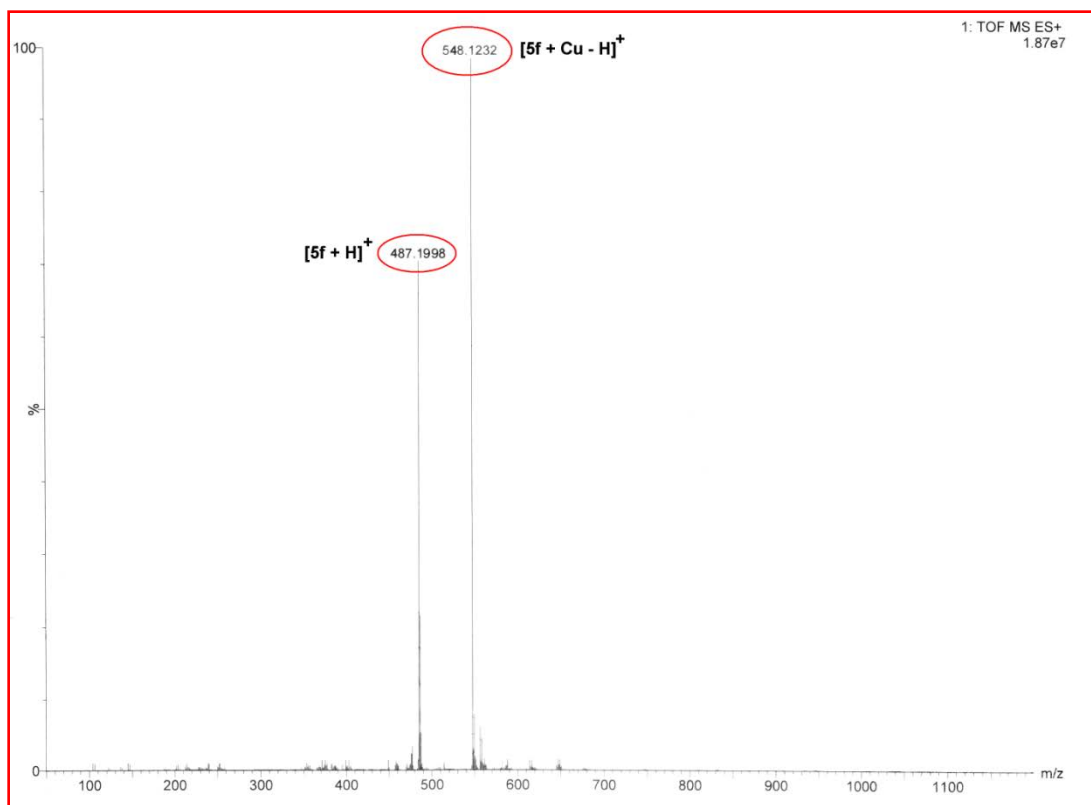
ESI-MS of compound **5c+Cu**



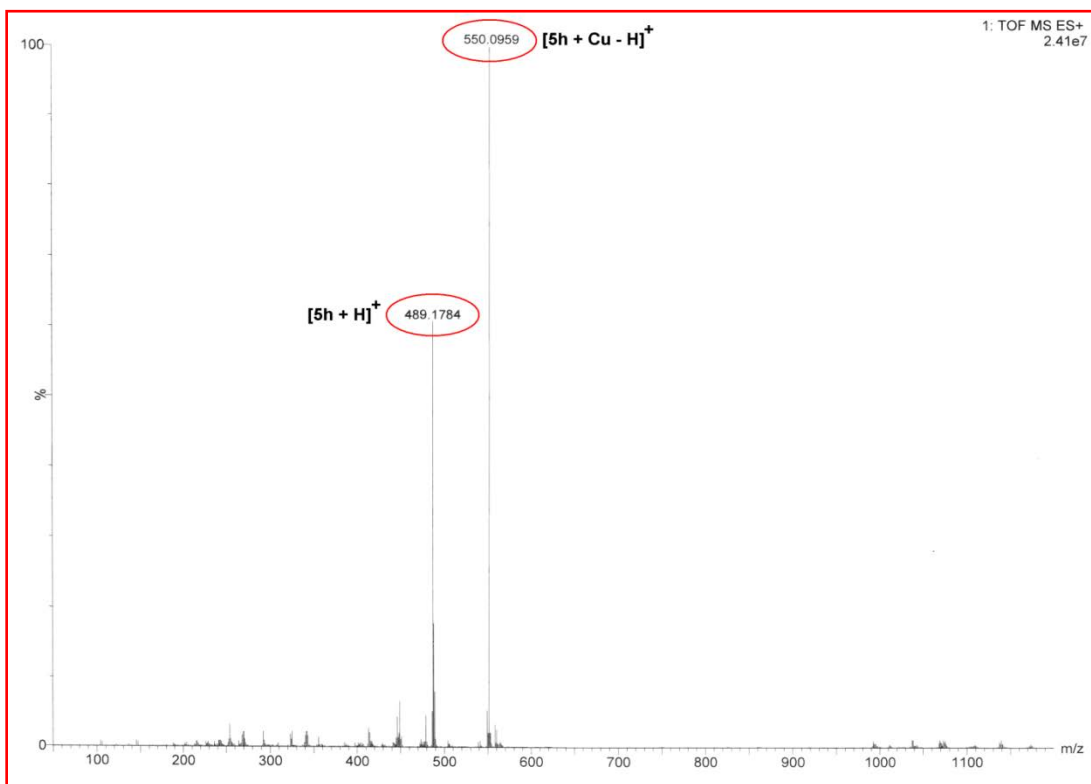
ESI-MS of compound **5d+Cu**



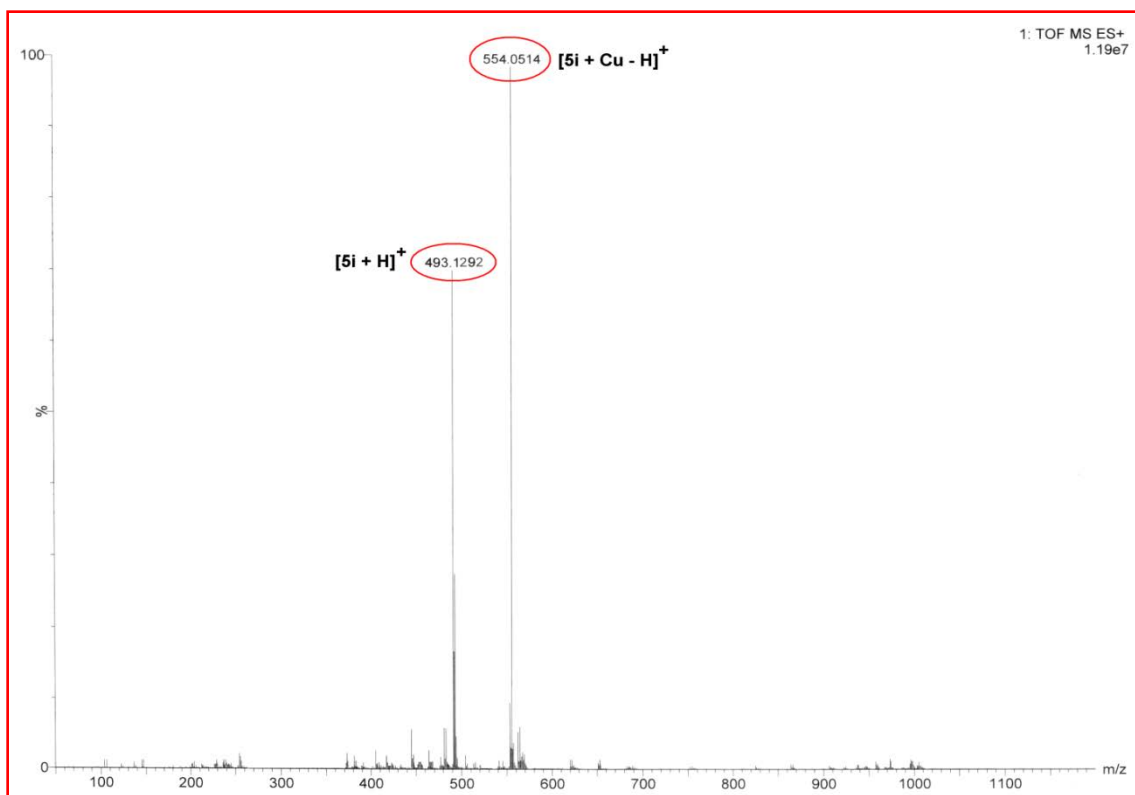
ESI-MS of compound **5e+Cu**



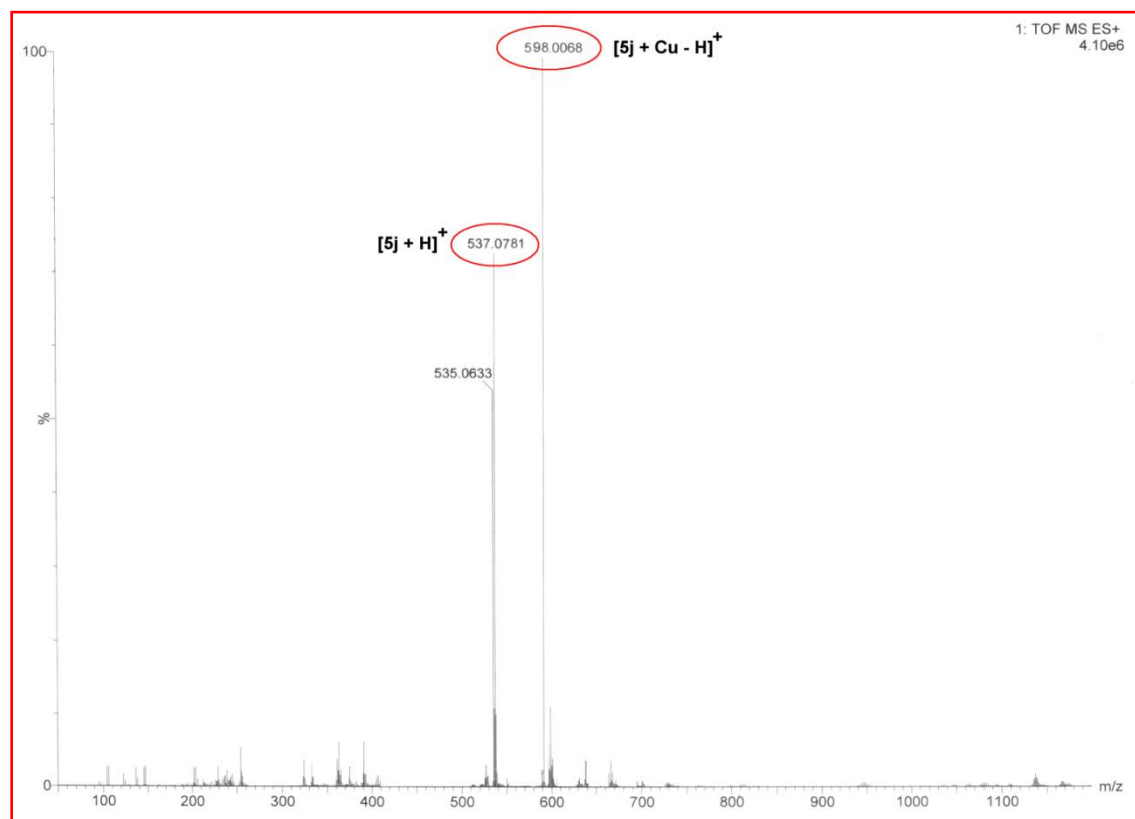
ESI-MS of compound **5f+Cu**



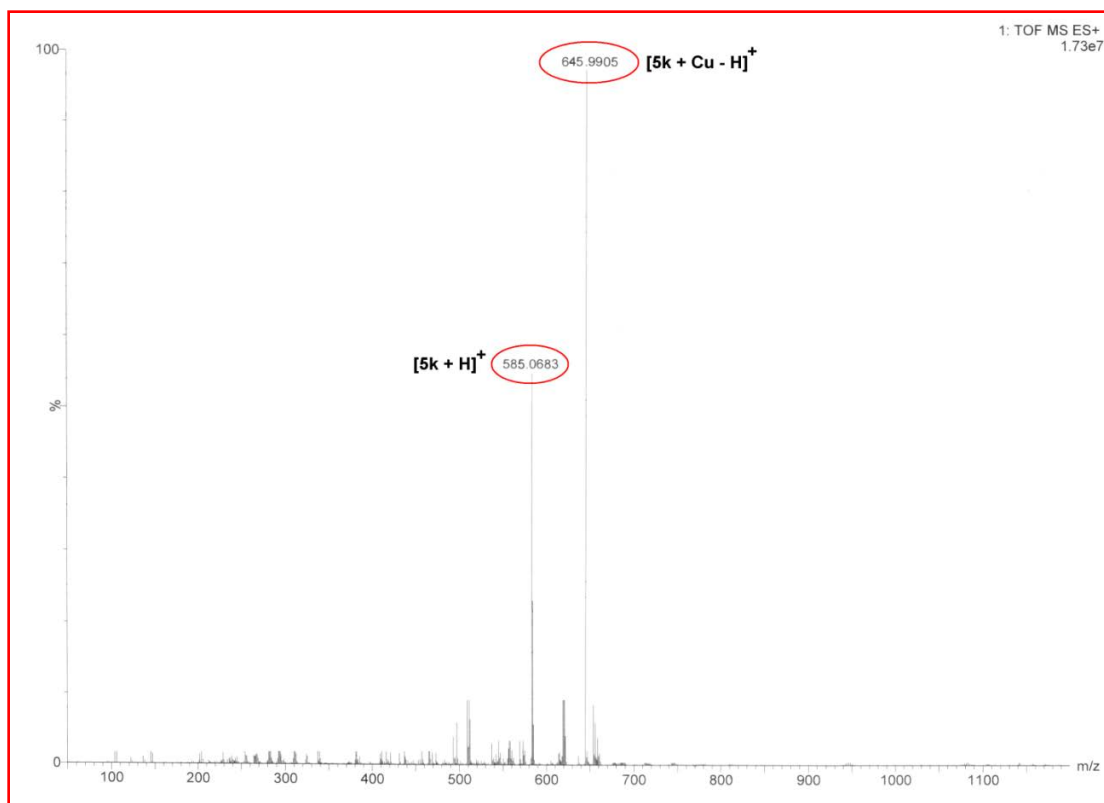
ESI-MS of compound **5h+Cu**



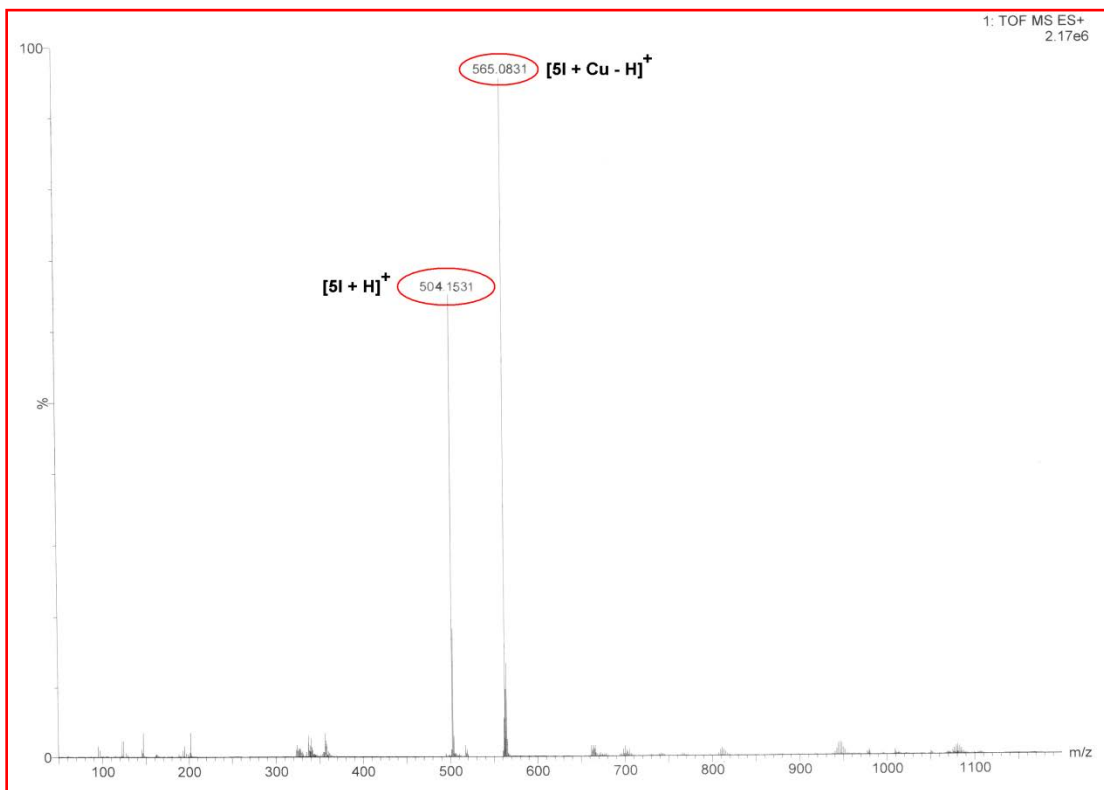
ESI-MS of compound **5i+Cu**



ESI-MS of compound **5j+Cu**



ESI-MS of compound **5k+Cu**



ESI-MS of compound **5l+Cu**

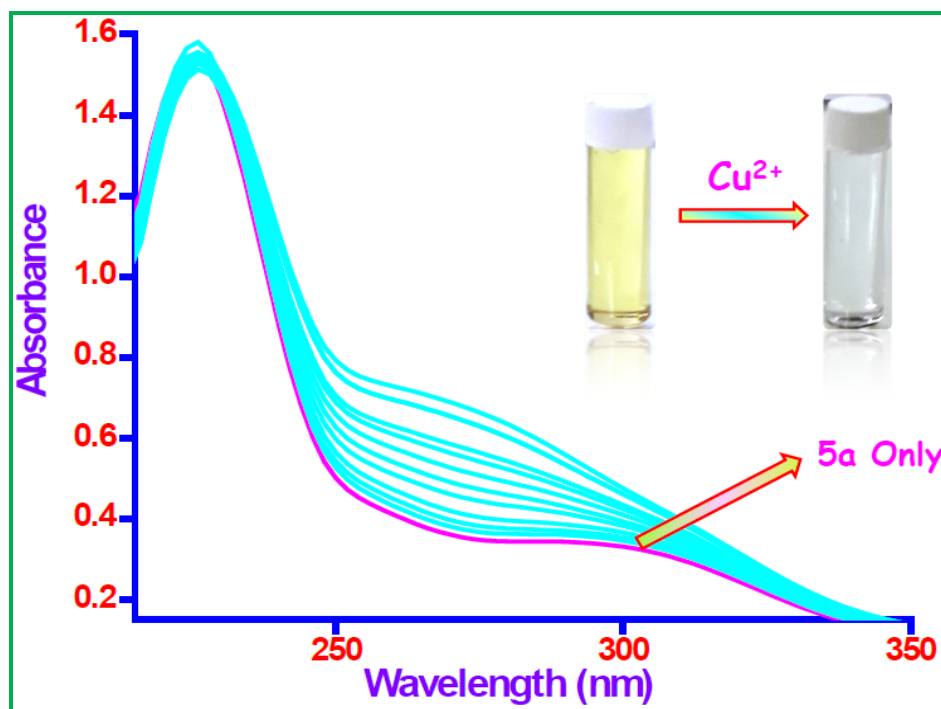


Figure S2. UV-vis spectra of **5a** (5×10^{-6} M) in DMSO/H₂O (1:9, v/v) HEPES buffer (pH = 7.4) solution in the presence of various concentrations of Cu²⁺ (0, 1, 2, 3, 4, 5, 6, 7, 8, 9 and 10) × 10⁻⁶ M. **Inset:** visual color change (yellow to colorless) observed with addition of Cu²⁺ ion to **5a** solution.

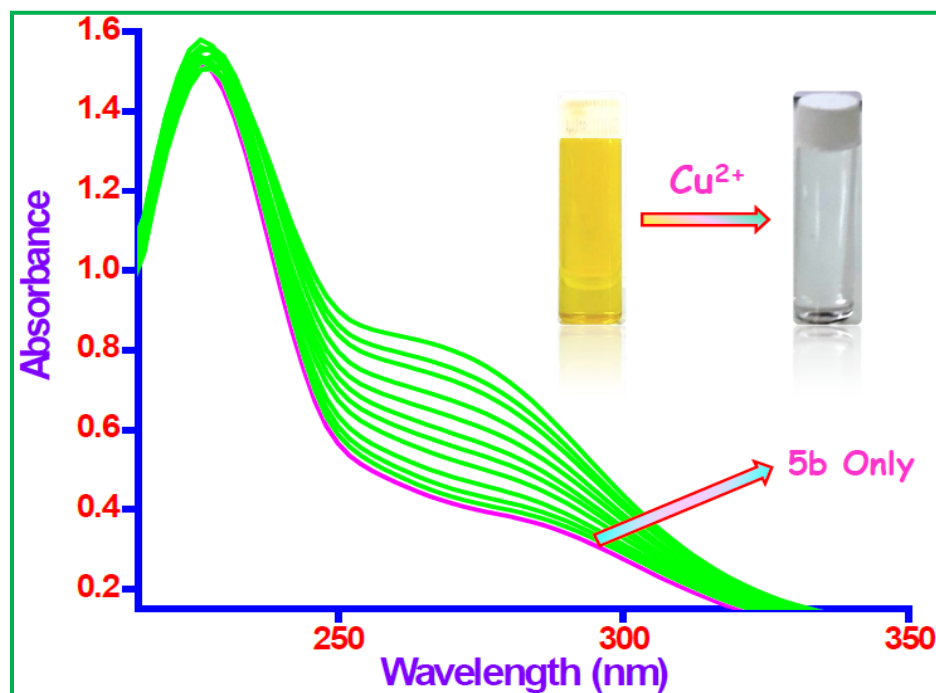


Figure S3. UV-vis spectra of **5b** (5×10^{-6} M) in DMSO/H₂O (1:9, v/v) HEPES buffer (pH = 7.4) solution in the presence of various concentrations of Cu²⁺ (0, 0.5, 1, 2, 3, 4, 5, 6, 7, 8, 9 and 10) × 10⁻⁶ M. **Inset:** visual color change (yellow to colorless) observed with addition of Cu²⁺ ion to **5b** solution.

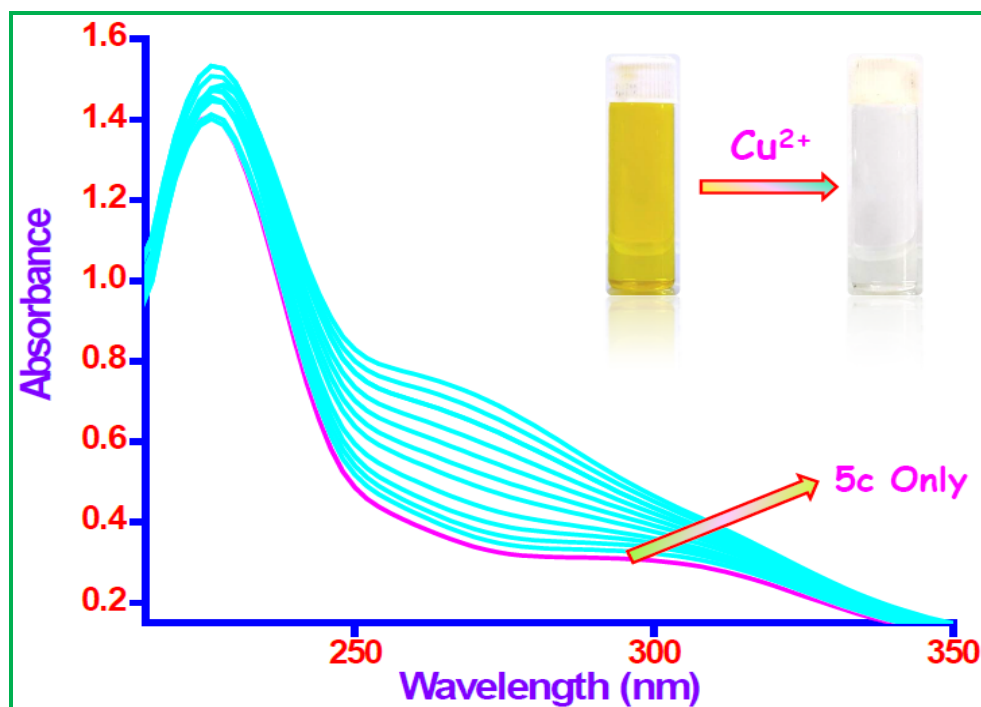


Figure S4. UV-vis spectra of **5c** (5×10^{-6} M) in DMSO/H₂O (1:9, v/v) HEPES buffer (pH = 7.4) solution in the presence of various concentrations of Cu²⁺ (0, 0.5, 1, 2, 3, 4, 5, 6, 7, 8, 9 and 10) $\times 10^{-6}$ M. **Inset:** visual color change (yellow to colorless) observed with addition of Cu²⁺ ion to **5c** solution.

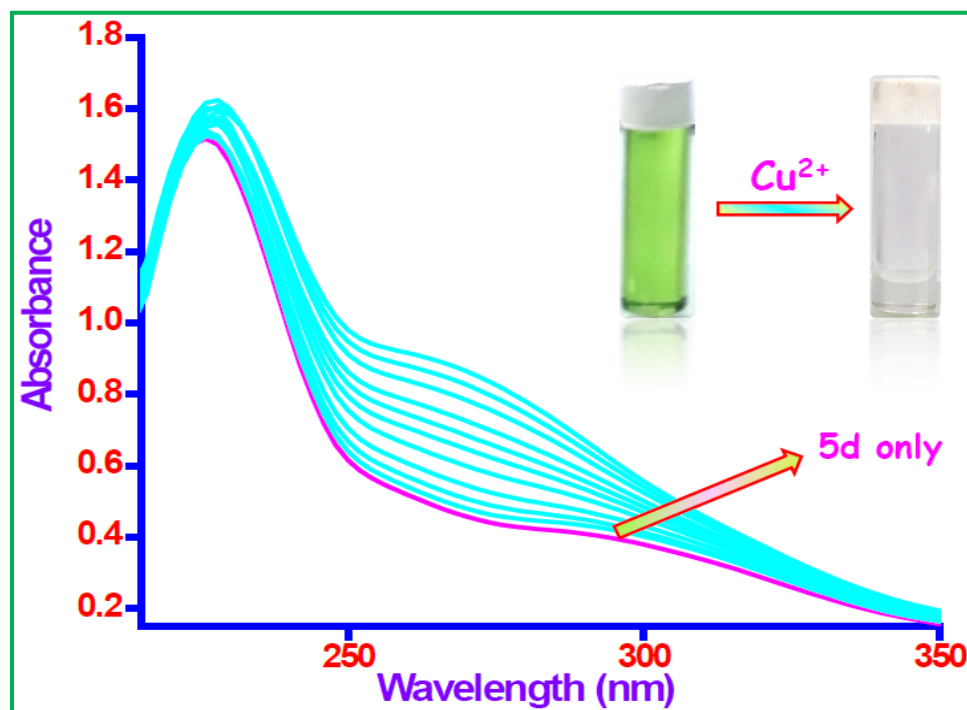


Figure S5. UV-vis spectra of **5d** (5×10^{-6} M) in DMSO/H₂O (1:9, v/v) HEPES buffer (pH = 7.4) solution in the presence of various concentrations of Cu²⁺ (0, 1, 2, 3, 4, 5, 6, 7, 8, 9 and 10) $\times 10^{-6}$ M. **Inset:** visual color change (green to colorless) observed with addition of Cu²⁺ ion to **5d** solution.

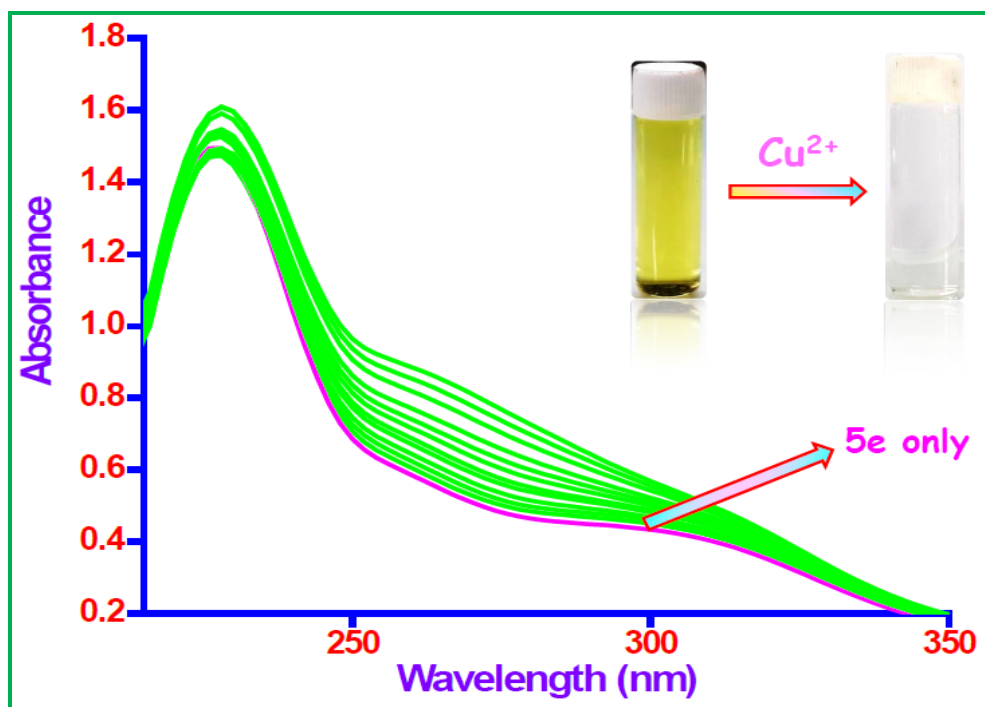


Figure S6. UV-vis spectra of **5e** (5×10^{-6} M) in DMSO/H₂O (1:9, v/v) HEPES buffer (pH = 7.4) solution in the presence of various concentrations of Cu²⁺ (0, 0.5, 1, 2, 3, 4, 5, 6, 7, 8, 9 and 10) × 10⁻⁶ M. **Inset:** visual color change (yellow to colorless) observed with addition of Cu²⁺ ion to **5e** solution.

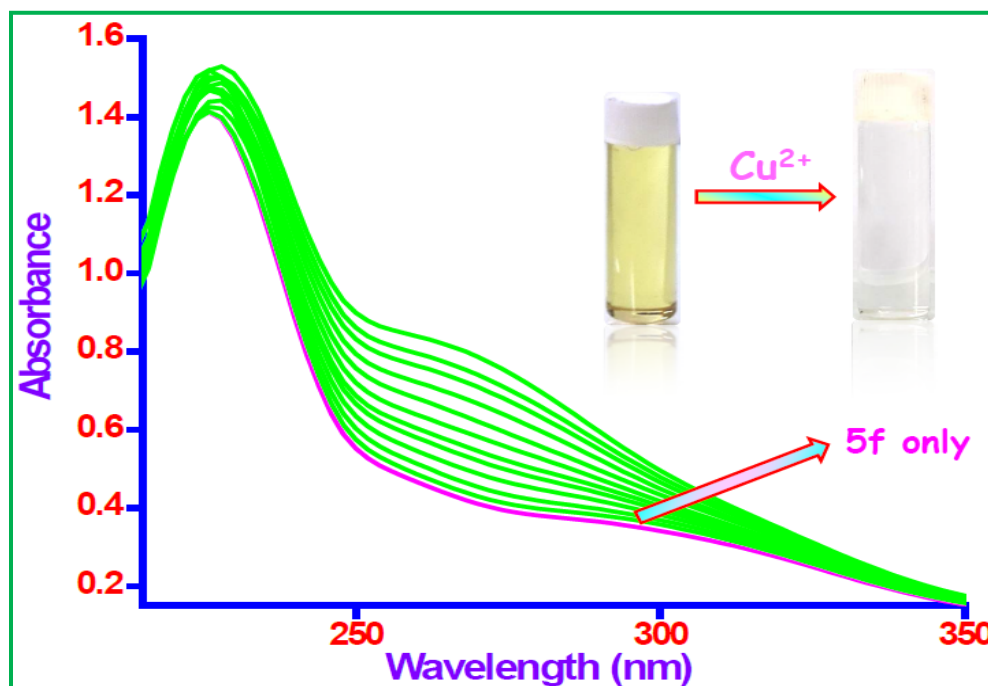


Figure S7. UV-vis spectra of **5f** (5×10^{-6} M) in DMSO/H₂O (1:9, v/v) HEPES buffer (pH = 7.4) solution in the presence of various concentrations of Cu²⁺ (0, 0.5, 1, 2, 3, 4, 5, 6, 7, 8, 9 and 10) × 10⁻⁶ M. **Inset:** visual color change (yellow to colorless) observed with addition of Cu²⁺ ion to **5f** solution.

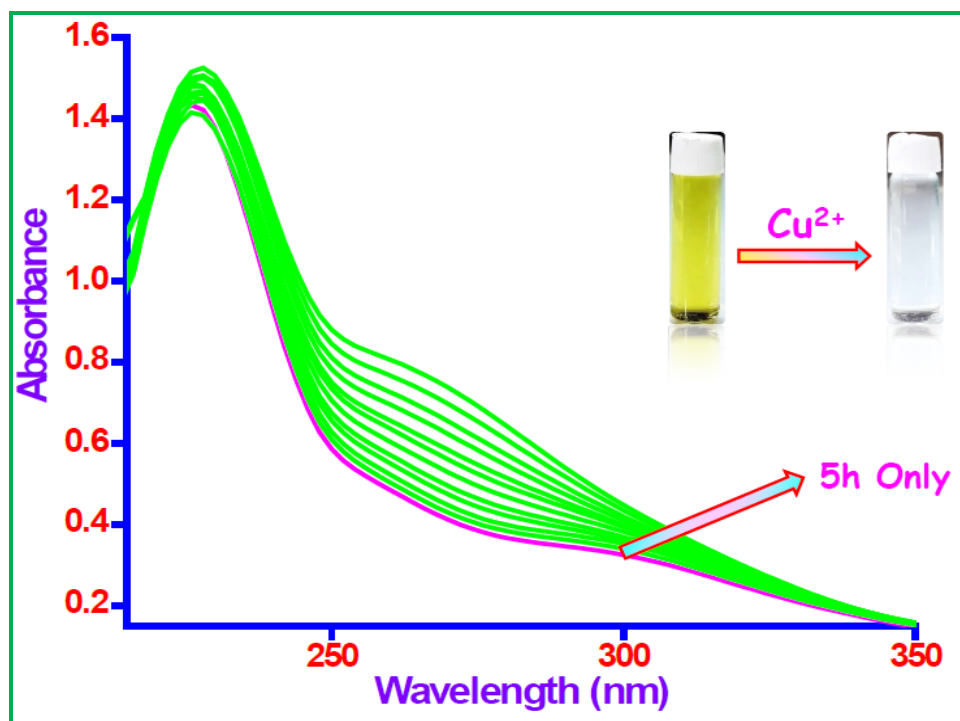


Figure S8. UV-vis spectra of **5h** (5×10^{-6} M) in DMSO/H₂O (1:9, v/v) HEPES buffer (pH = 7.4) solution in the presence of various concentrations of Cu²⁺ (0, 0.5, 1, 2, 3, 4, 5, 6, 7, 8, 9 and 10) × 10⁻⁶ M. **Inset:** visual color change (yellow to colorless) observed with addition of Cu²⁺ ion to **5h** solution.

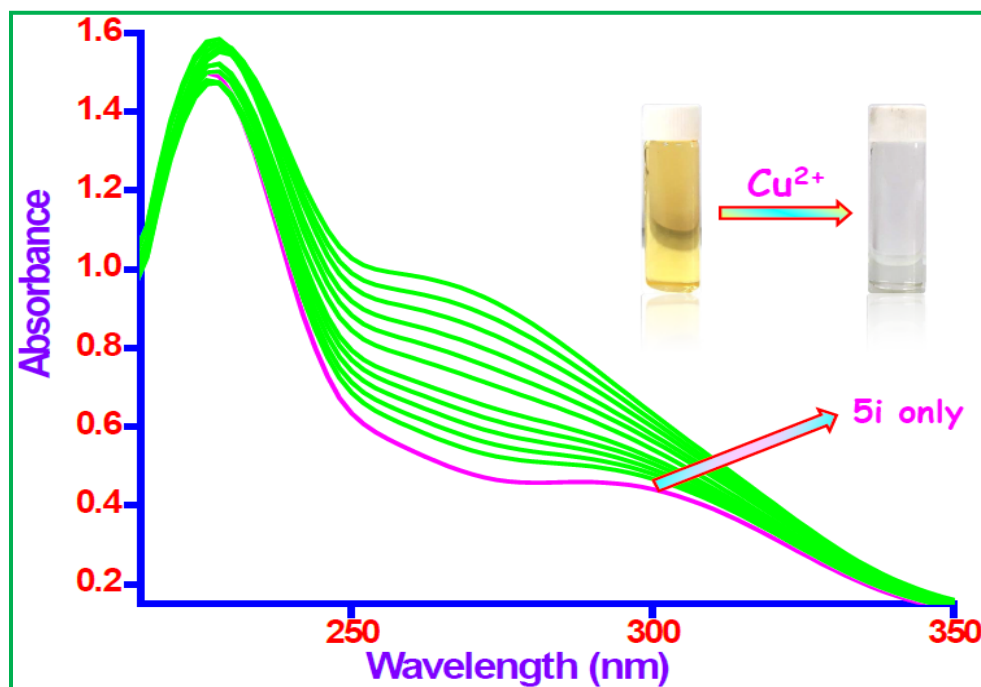


Figure S9. UV-vis spectra of **5i** (5×10^{-6} M) in DMSO/H₂O (1:9, v/v) HEPES buffer (pH = 7.4) solution in the presence of various concentrations of Cu²⁺ (0, 0.5, 1, 2, 3, 4, 5, 6, 7, 8, 9 and 10) × 10⁻⁶ M. **Inset:** visual color change (yellow to colorless) observed with addition of Cu²⁺ ion to **5i** solution.

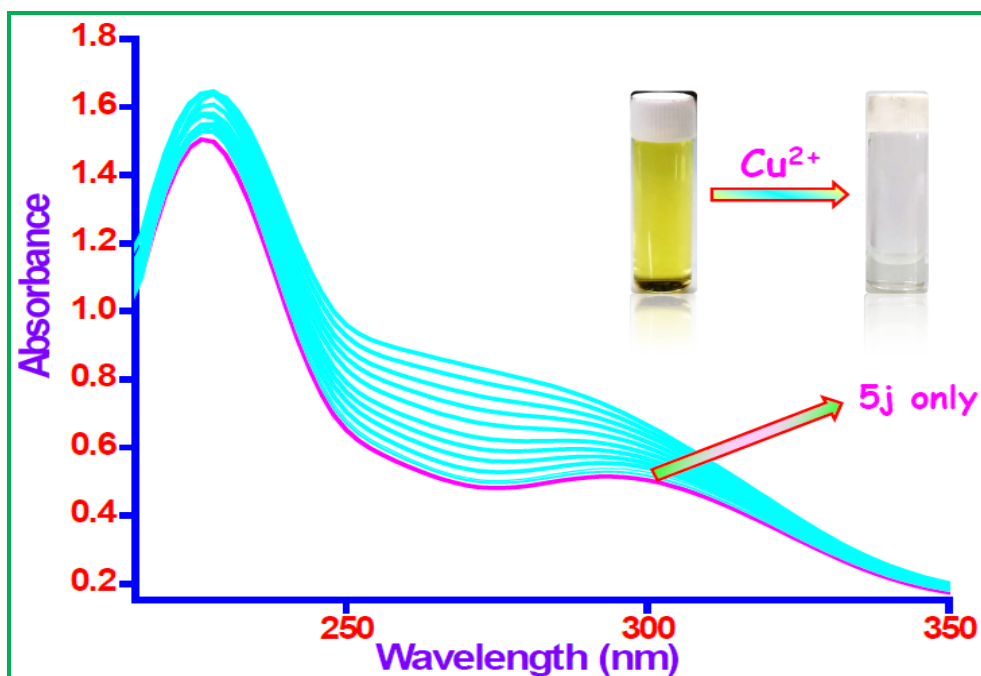


Figure S10. UV-vis spectra of **5j** (5×10^{-6} M) in DMSO/H₂O (1:9, v/v) HEPES buffer (pH = 7.4) solution in the presence of various concentrations of Cu²⁺ (0, 1, 2, 3, 4, 5, 6, 7, 8, 9 and 10) $\times 10^{-6}$ M. **Inset:** visual color change (yellow to colorless) observed with addition of Cu²⁺ ion to **5j** solution.

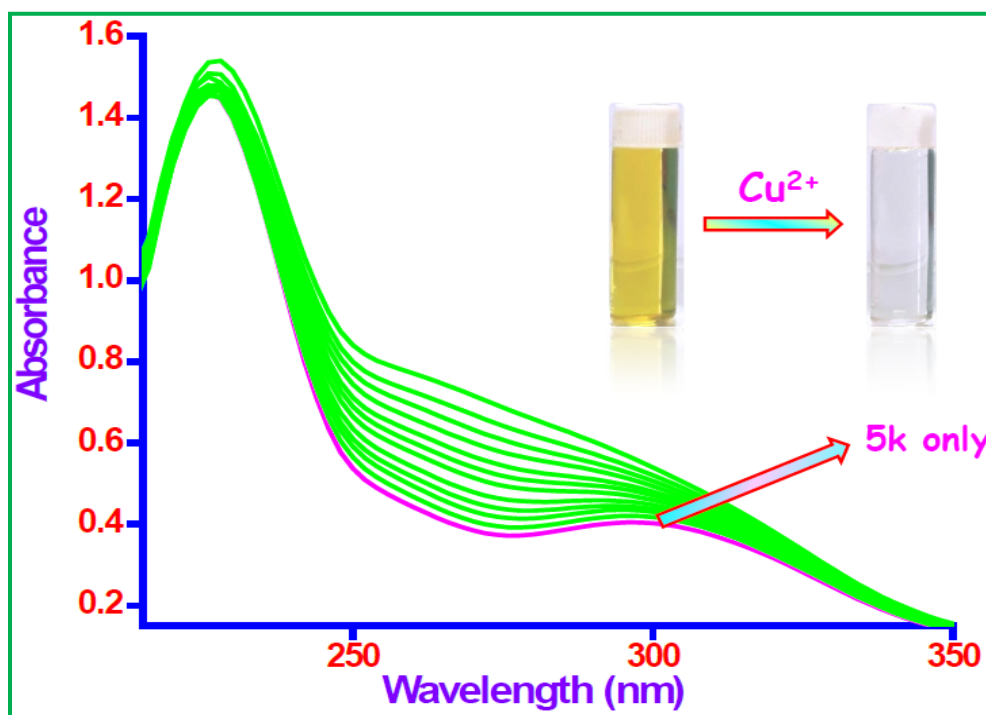


Figure S11. UV-vis spectra of **5k** (5×10^{-6} M) in DMSO/H₂O (1:9, v/v) HEPES buffer (pH = 7.4) solution in the presence of various concentrations of Cu²⁺ (0, 0.5, 1, 2, 3, 4, 5, 6, 7, 8, 9 and 10) $\times 10^{-6}$ M. **Inset:** visual color change (yellow to colorless) observed with addition of Cu²⁺ ion to **5k** solution.

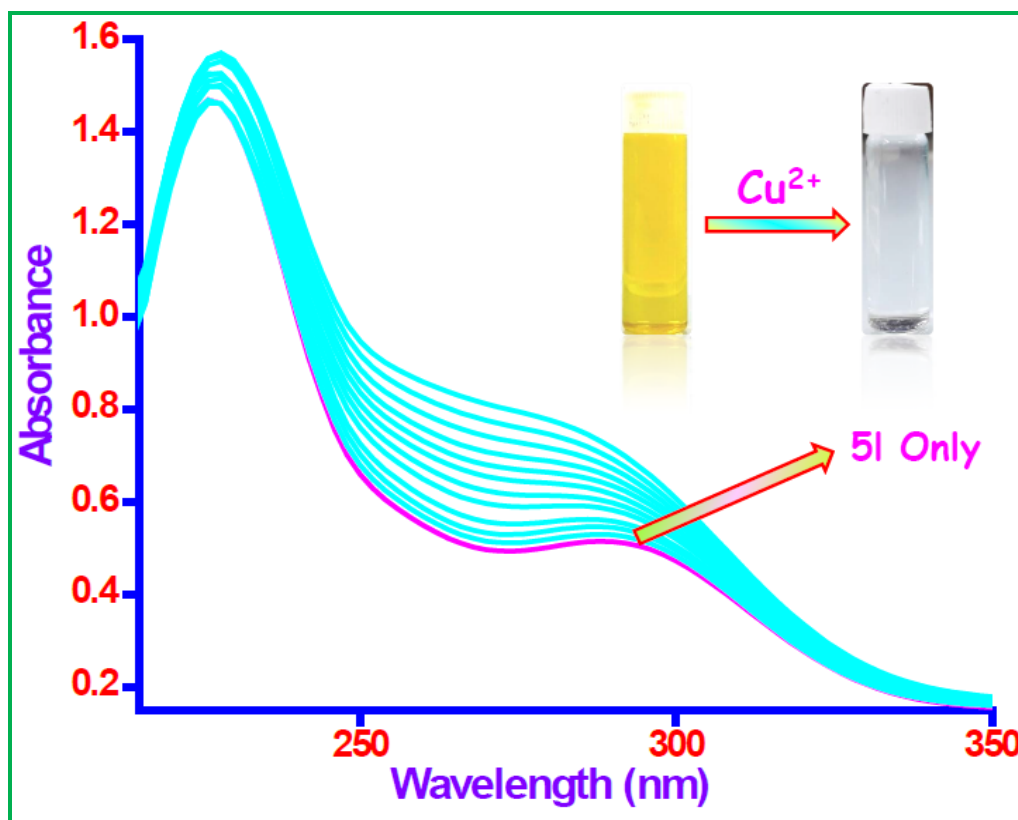


Figure S12. UV-vis spectra of **5I** (5×10^{-6} M) in DMSO/H₂O (1:9, v/v) HEPES buffer (pH = 7.4) solution in the presence of various concentrations of Cu²⁺ (0, 0.5, 1, 2, 3, 4, 5, 6, 7, 8, 9 and 10) $\times 10^{-6}$ M. **Inset:** visual color change (yellow to colorless) observed with addition of Cu²⁺ ion to **5I** solution.

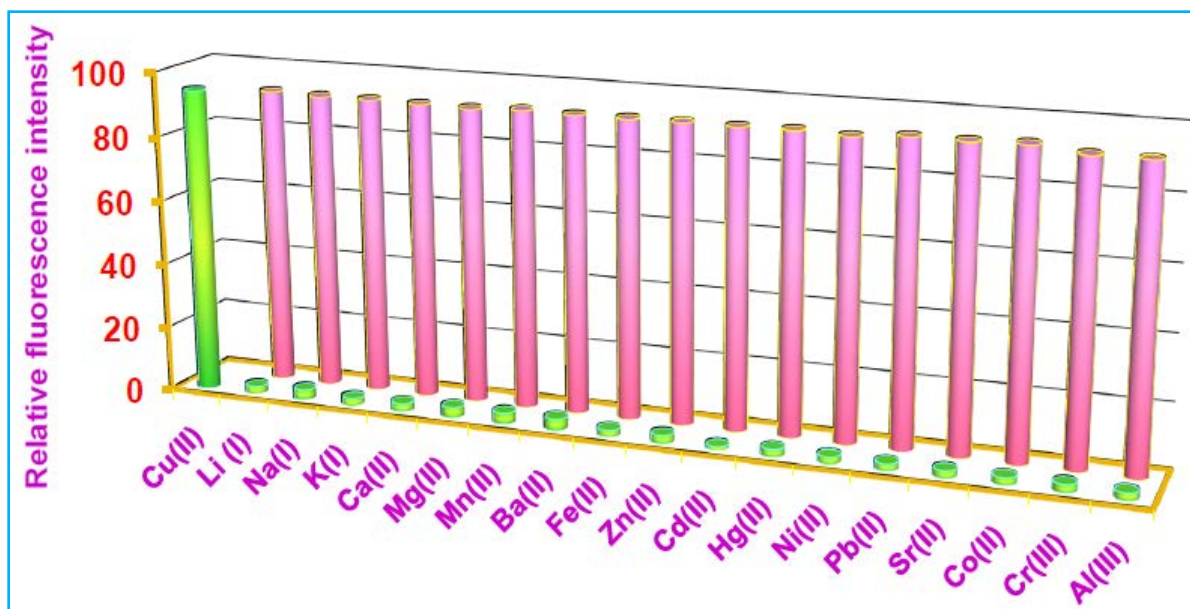


Figure S13. Fluorescence Quenching Efficiency (FQE), $[\{(F_0 - F)/F_0\} \times 100]$ of **5d** (5×10^{-6} M) in the presence of 4 equiv. of different cations except 2 equiv. of Cu^{2+} in solution [the green bar portion]. Fluorescence Quenching Efficiency (FQE) of a mixture of **5d** (5×10^{-6} M) with other metal ions (20×10^{-6} M) followed by the addition of Cu^{2+} (10×10^{-6} M) to the DMSO/ H_2O (1:9, v/v) HEPES buffer (pH = 7.4) solution [$\lambda_{\text{ex}} = 375.7$ nm, $\lambda_{\text{em}} = 493.5$ nm].

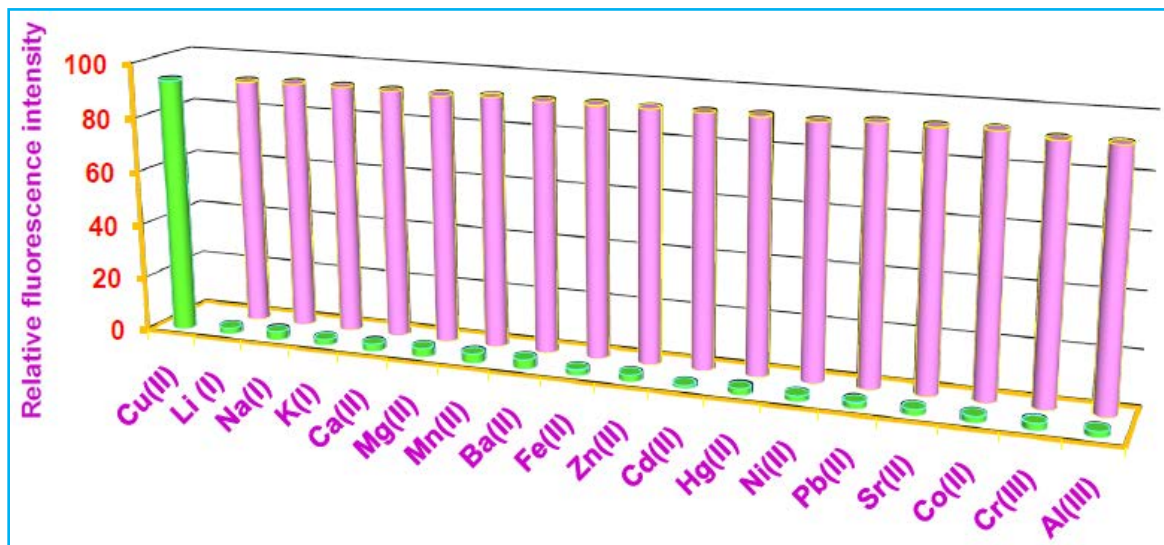


Figure S14. Fluorescence Quenching Efficiency (FQE), $[\{(F_0 - F)/F_0\} \times 100]$ of **5f** (5×10^{-6} M) in the presence of 4 equiv. of different cations except 2 equiv. of Cu^{2+} in solution [the green bar portion]. Fluorescence Quenching Efficiency (FQE) of a mixture of **5f** (5×10^{-6} M) with other metal ions (20×10^{-6} M) followed by the addition of Cu^{2+} (10×10^{-6} M) to the DMSO/ H_2O (1:9, v/v) HEPES buffer (pH = 7.4) solution [$\lambda_{\text{ex}} = 310.9$ nm, $\lambda_{\text{em}} = 491.7$ nm].

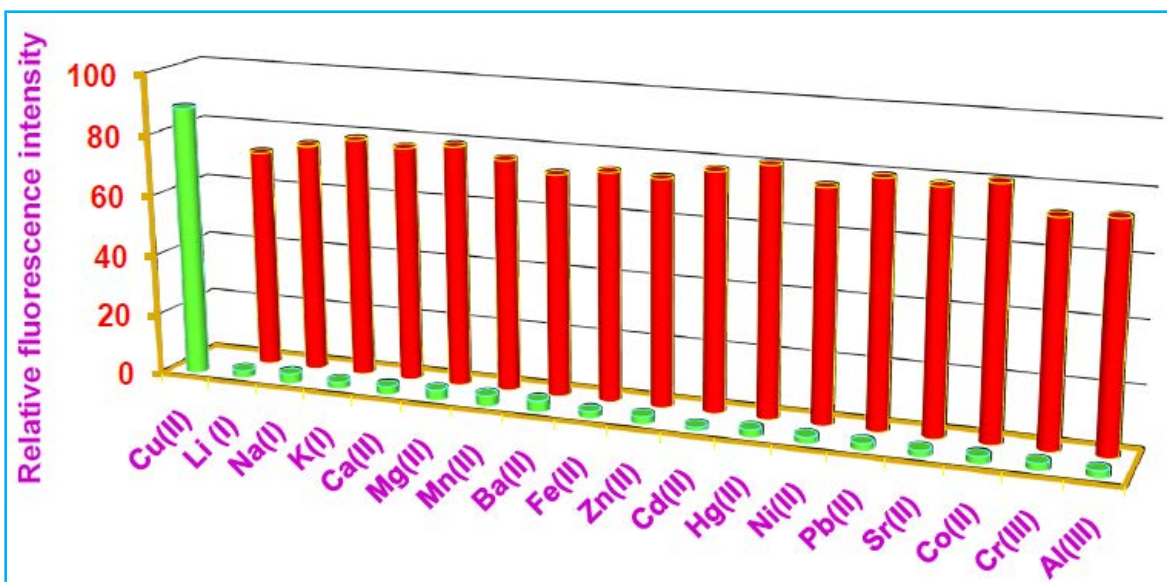


Figure S15. Fluorescence Quenching Efficiency (FQE), $\left[\frac{F_0 - F}{F_0}\right] \times 100$ of **5h** (5×10^{-6} M) in the presence of 4 equiv. of different cations except 2 equiv. of Cu^{2+} in solution [the green bar portion]. Fluorescence Quenching Efficiency (FQE) of a mixture of **5h** (5×10^{-6} M) with other metal ions (20×10^{-6} M) followed by the addition of Cu^{2+} (10×10^{-6} M) to the DMSO/ H_2O (1:9, v/v) HEPES buffer (pH = 7.4) solution [the red bar portion] ($\lambda_{\text{ex}} = 308.5$ nm, $\lambda_{\text{em}} = 498.7$ nm).

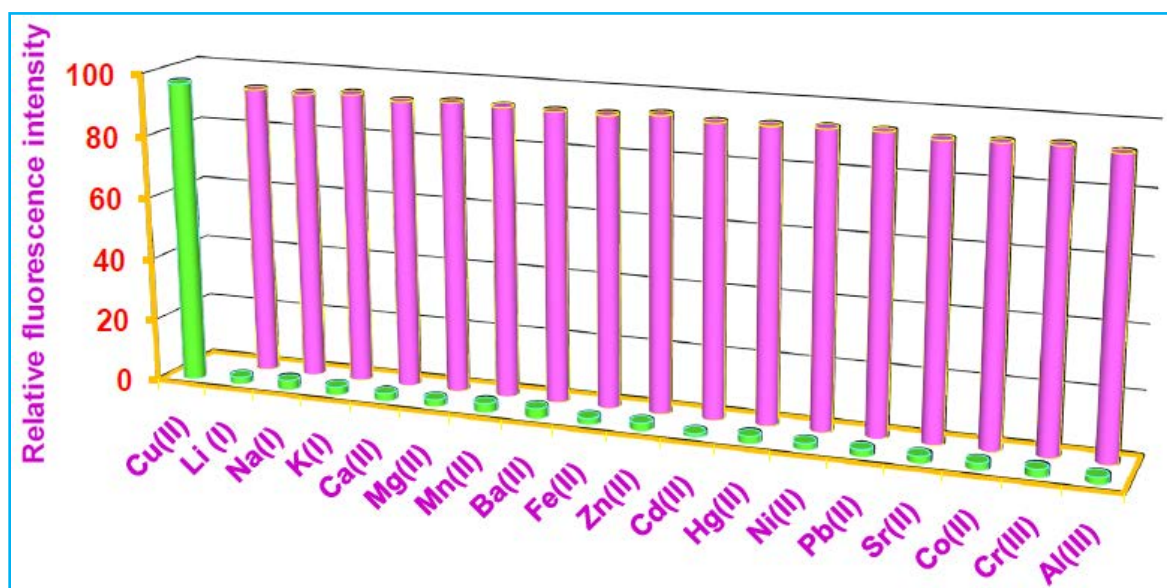


Figure S16. Fluorescence Quenching Efficiency (FQE), $\left[\frac{F_0 - F}{F_0}\right] \times 100$ of **5j** (5×10^{-6} M) in the presence of 4 equiv. of different cations except 2 equiv. of Cu^{2+} in solution [the green bar portion]. Fluorescence Quenching Efficiency (FQE) of a mixture of **5j** (5×10^{-6} M) with other metal ions (20×10^{-6} M) followed by the addition of Cu^{2+} (10×10^{-6} M) to the DMSO/ H_2O (1:9, v/v) HEPES buffer (pH = 7.4) solution [the pink bar portion] ($\lambda_{\text{ex}} = 302.4$ nm, $\lambda_{\text{em}} = 497.8$ nm).

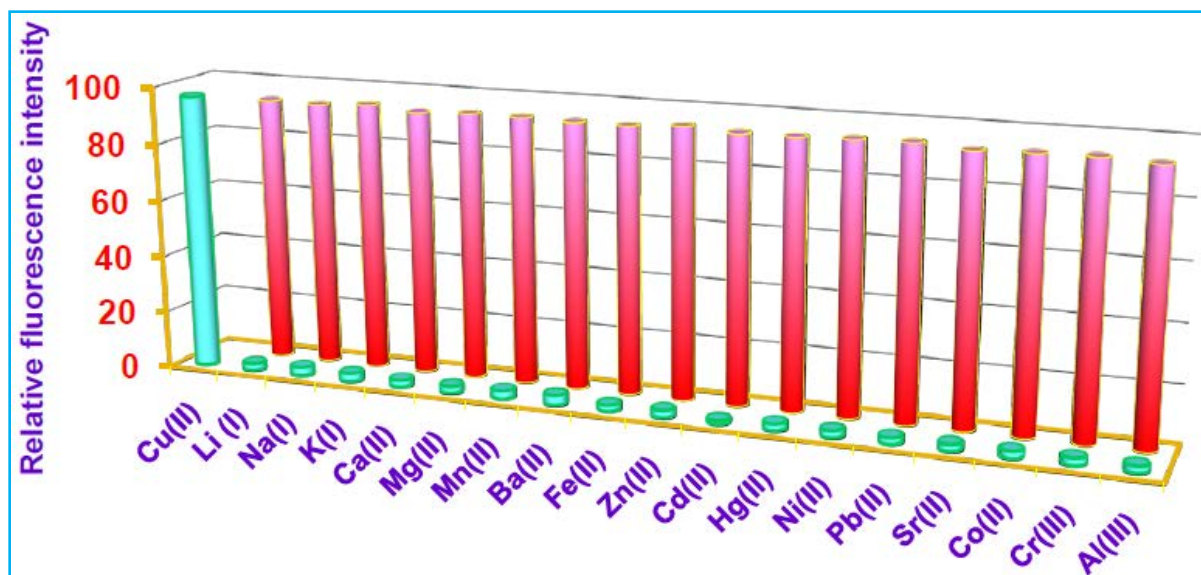


Figure S17. Fluorescence Quenching Efficiency (FQE), $[(F_0 - F)/F_0] \times 100$ of **5k** (5×10^{-6} M) in the presence of 4 equiv. of different cations except 2 equiv. of Cu^{2+} in solution [the cyan bar portion]. Fluorescence Quenching Efficiency (FQE) of a mixture of **5k** (5×10^{-6} M) with other metal ions (20×10^{-6} M) followed by the addition of Cu^{2+} (10×10^{-6} M) to the DMSO/ H_2O (1:9, v/v) HEPES buffer (pH = 7.4) solution [the red bar portion] ($\lambda_{\text{ex}} = 312.5$ nm, $\lambda_{\text{em}} = 503.5$ nm).

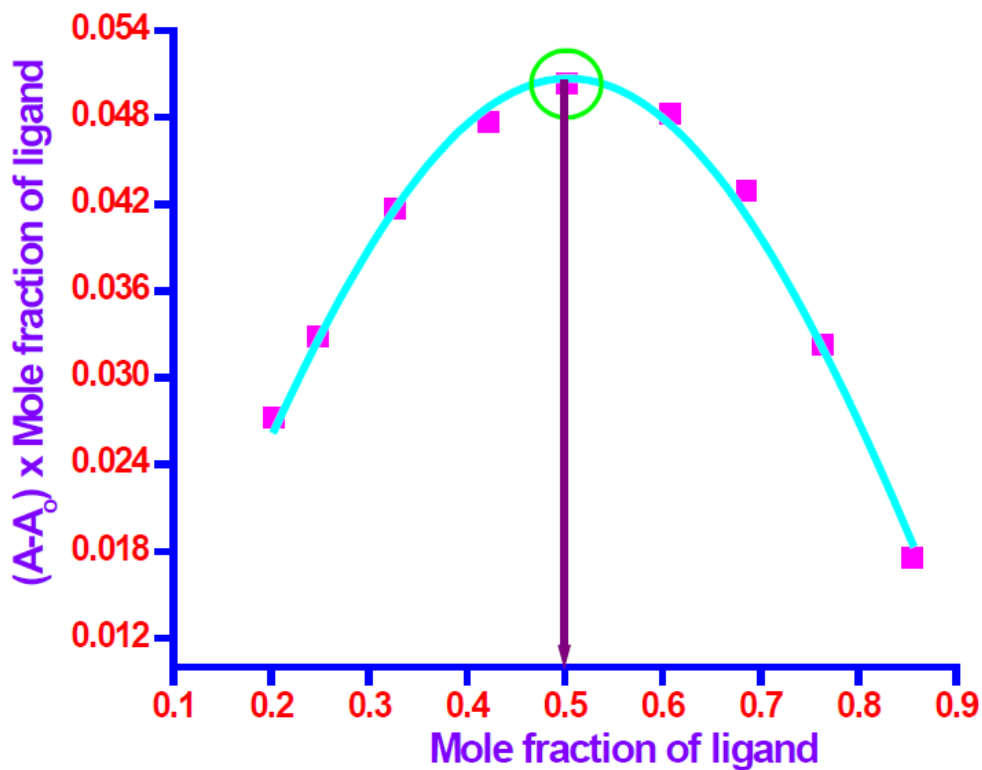


Figure S18. Job's plot for determination of stoichiometry of Cu^{2+} : **5a** complex in solution.

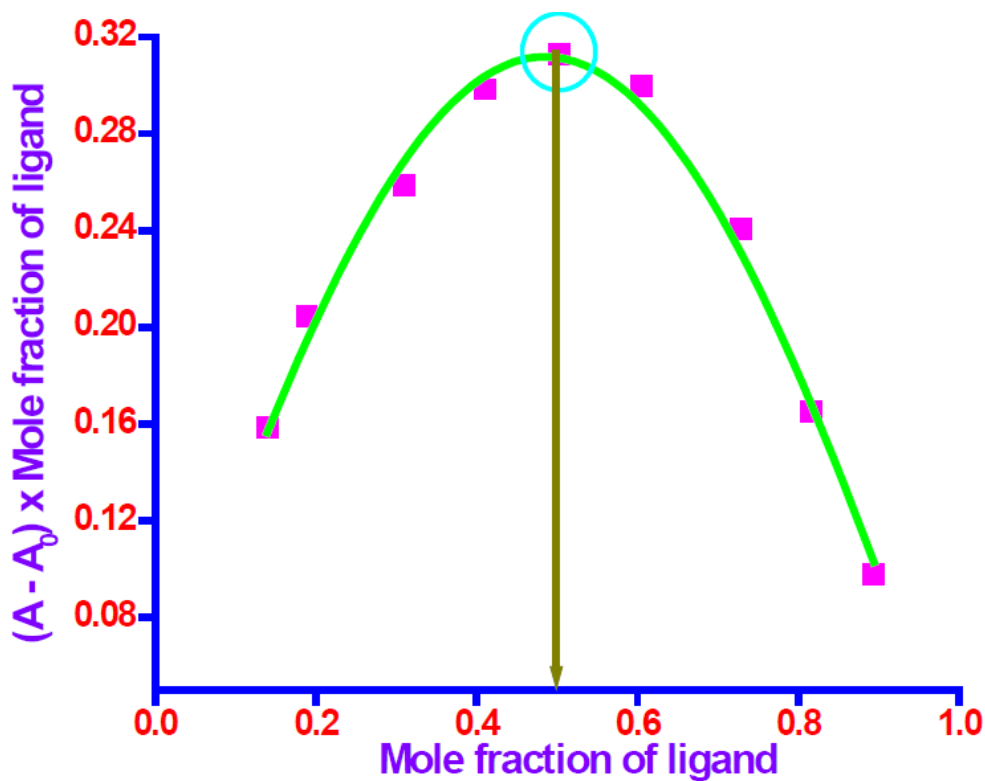


Figure S19. Job's plot for determination of stoichiometry of Cu^{2+} : **5b** complex in solution.

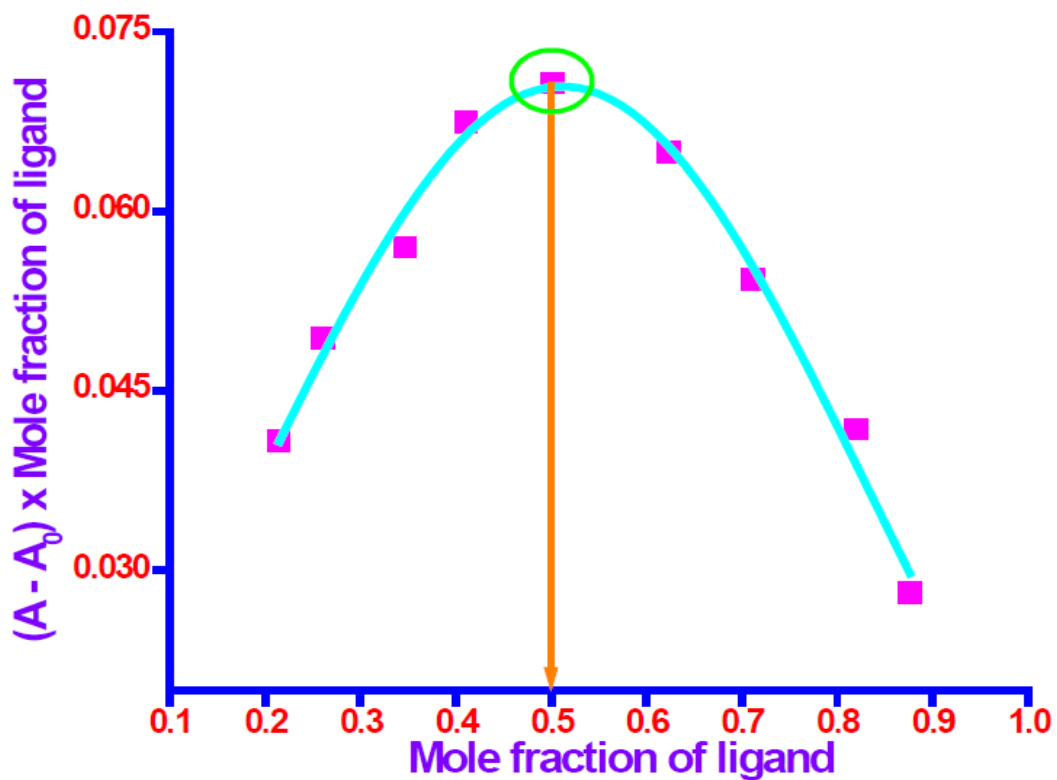


Figure S20. Job's plot for determination of stoichiometry of $\text{Cu}^{2+} : 5\text{c}$ complex in solution.

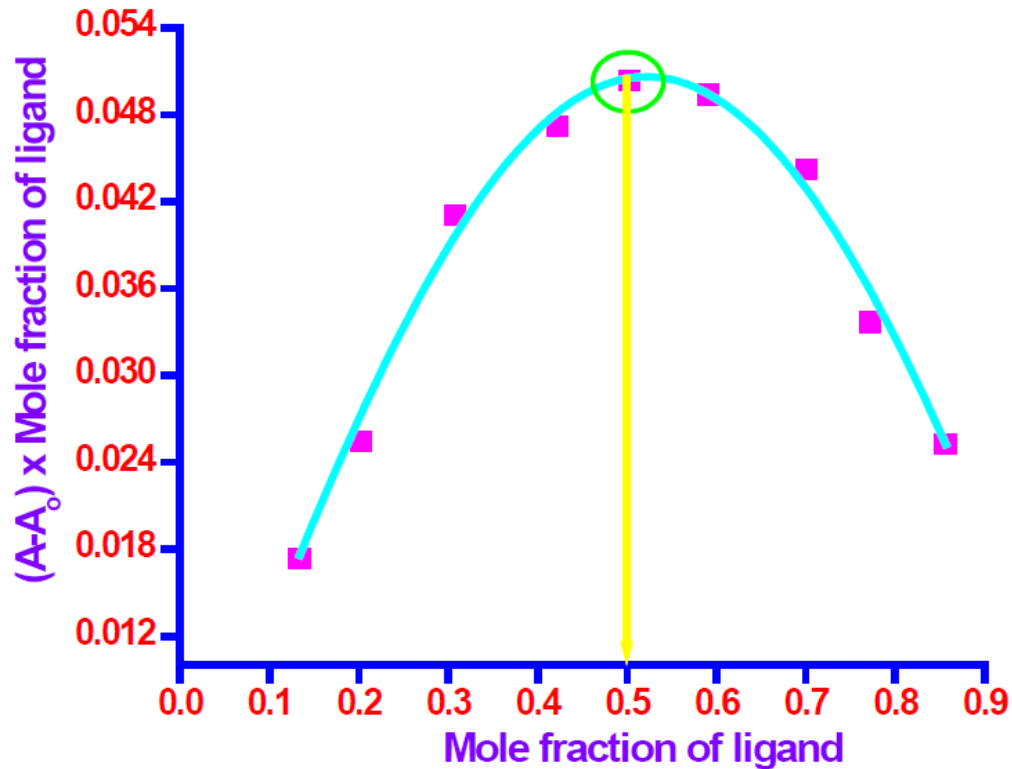


Figure S21. Job's plot for determination of stoichiometry of $\text{Cu}^{2+} : 5\text{d}$ complex in solution.

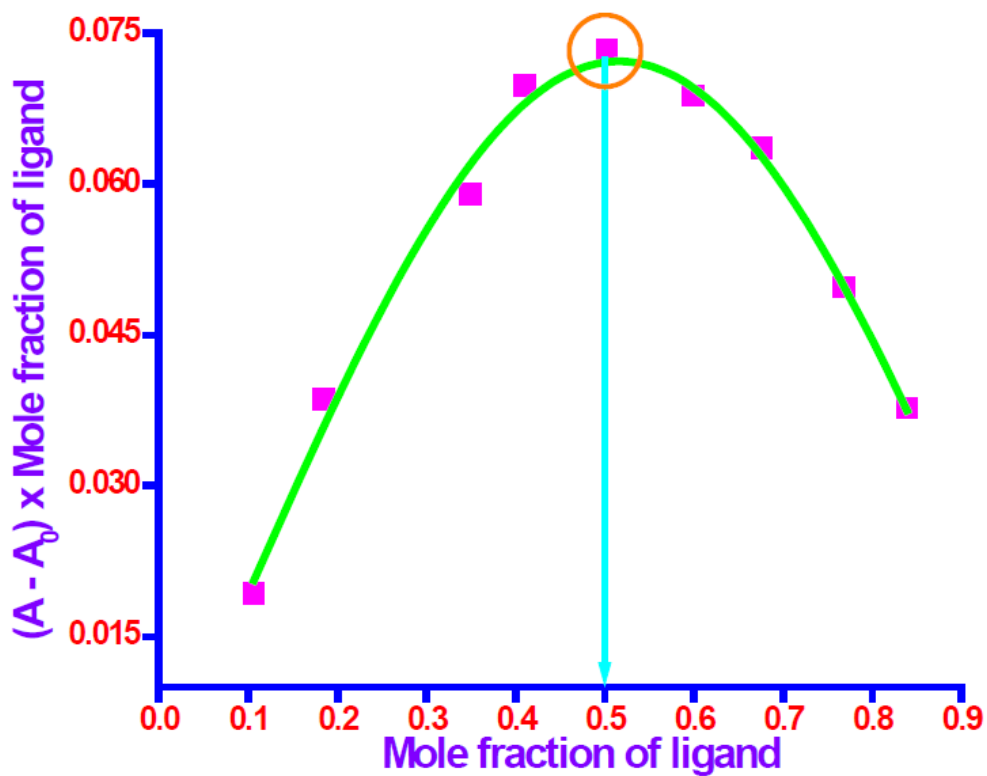


Figure S22. Job's plot for determination of stoichiometry of $\text{Cu}^{2+} : 5\text{e}$ complex in solution.

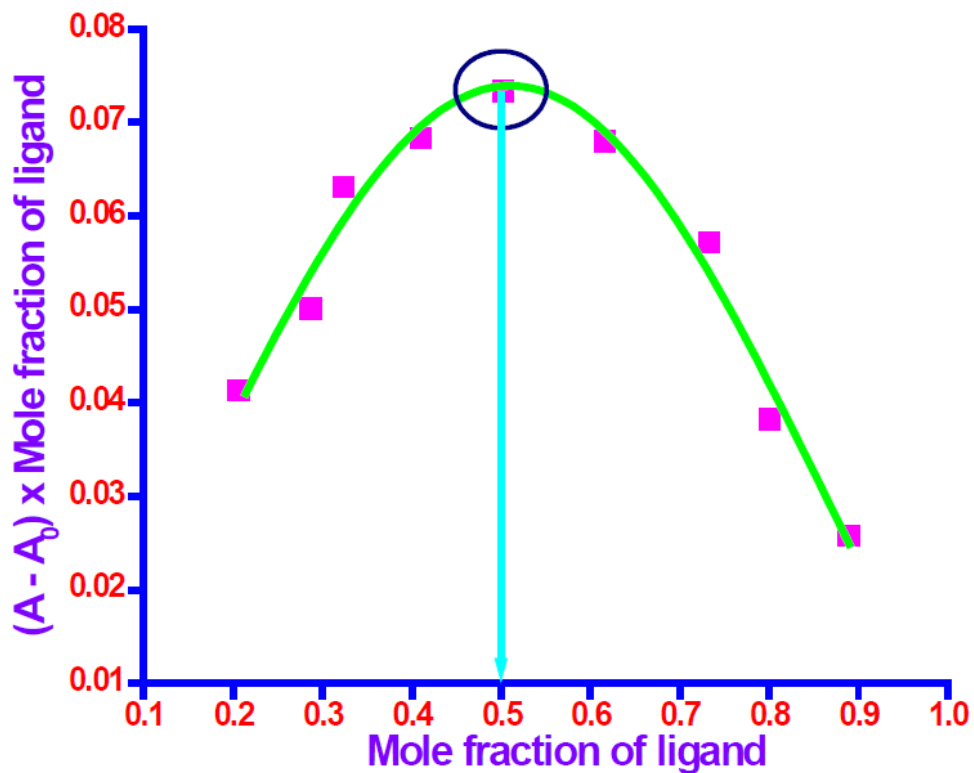


Figure S23. Job's plot for determination of stoichiometry of $\text{Cu}^{2+} : 5\text{f}$ complex in solution.

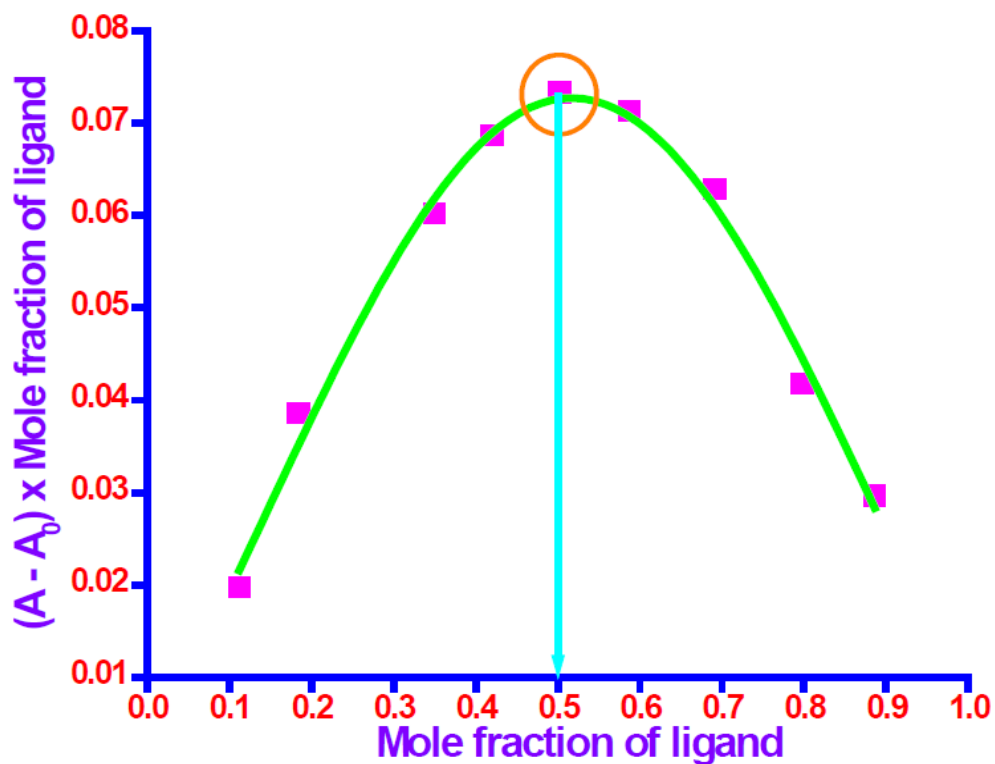


Figure S24. Job's plot for determination of stoichiometry of $\text{Cu}^{2+} : \mathbf{5h}$ complex in solution.

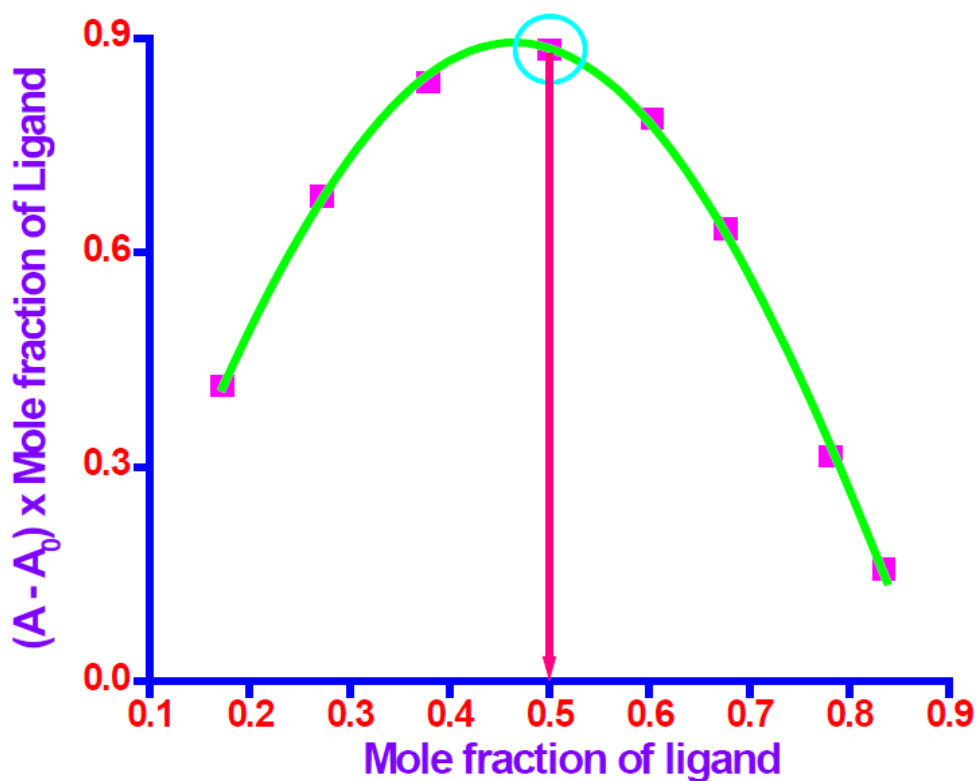


Figure S25. Job's plot for determination of stoichiometry of $\text{Cu}^{2+} : \mathbf{5i}$ complex in solution.

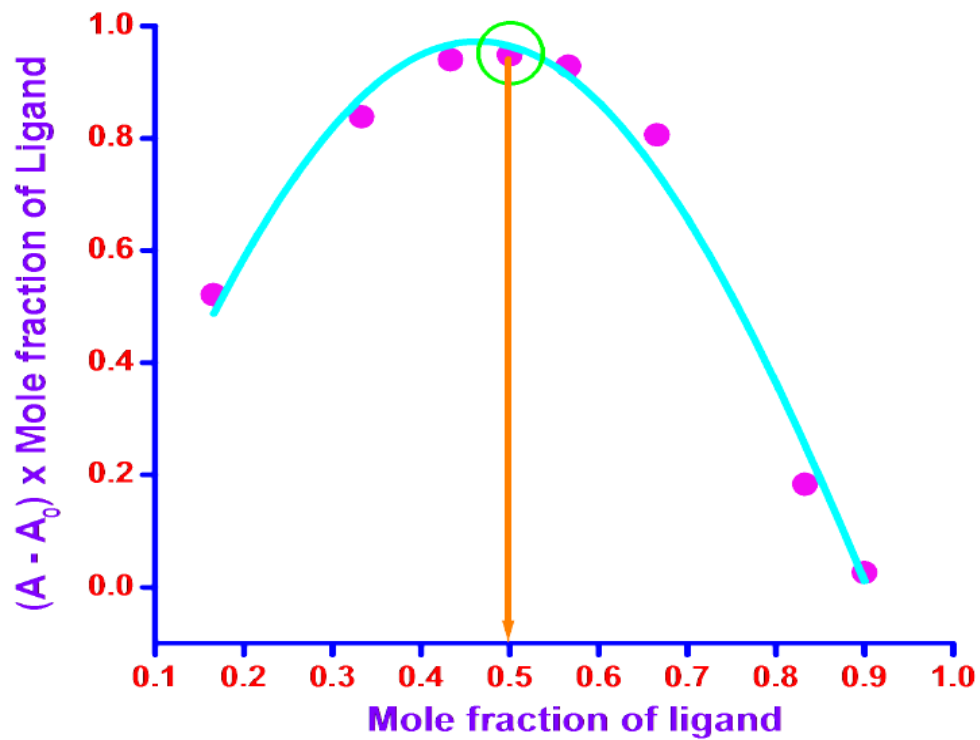


Figure S26. Job's plot for determination of stoichiometry of $\text{Cu}^{2+} : \mathbf{5j}$ complex in solution.

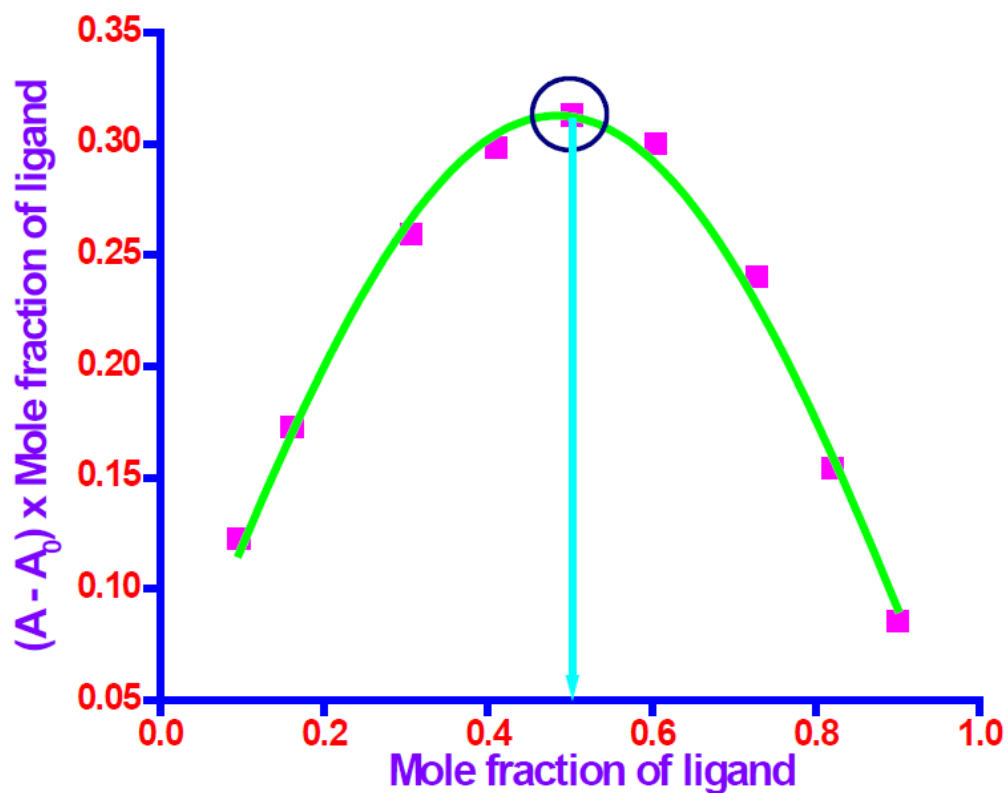


Figure S27. Job's plot for determination of stoichiometry of $\text{Cu}^{2+} : \mathbf{5k}$ complex in solution.

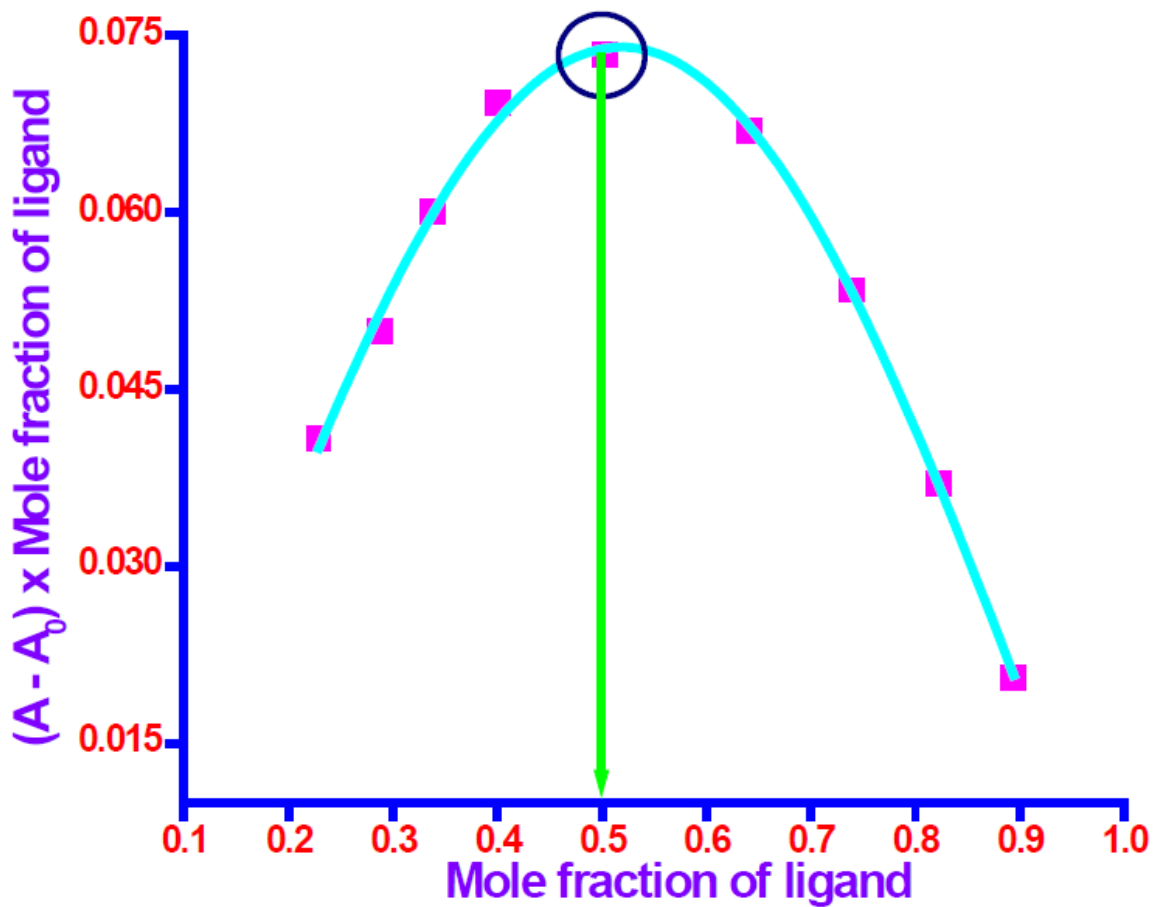


Figure S28. Job's plot for determination of stoichiometry of $\text{Cu}^{2+} : 5\text{I}$ complex in solution.

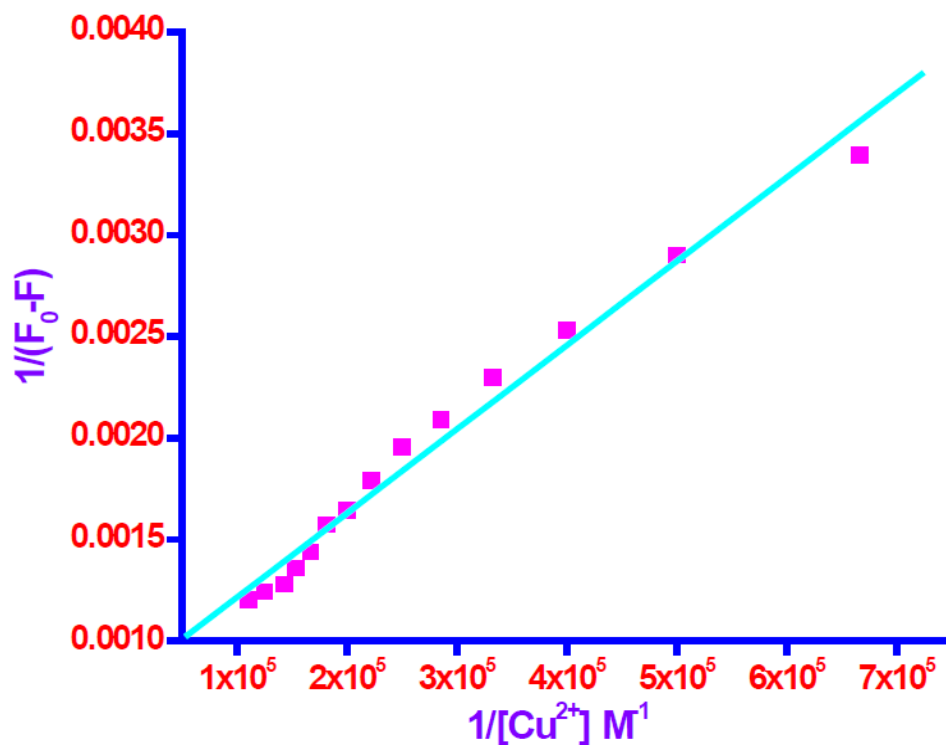


Figure S29. Benesi-Hildebrand plot $1 / (F_0 - F)$ vs. $1/[Cu^{2+}]$ for complexation between **5d** and Cu^{2+} derived from emission titration curve.

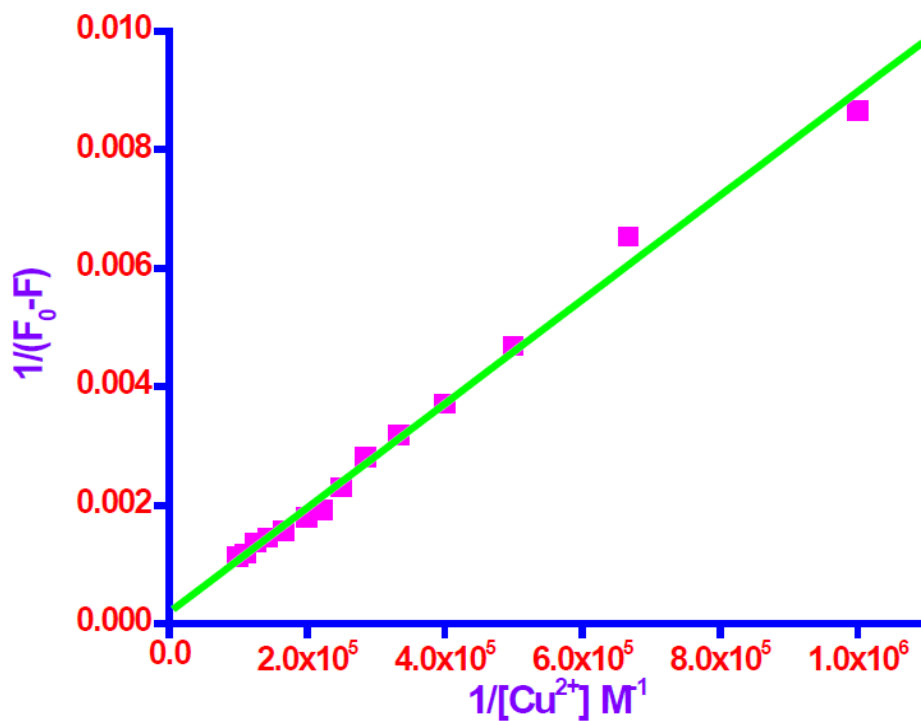


Figure S30. Benesi-Hildebrand plot $1 / (F_0 - F)$ vs. $1/[Cu^{2+}]$ for complexation between **5f** and Cu^{2+} derived from emission titration curve.

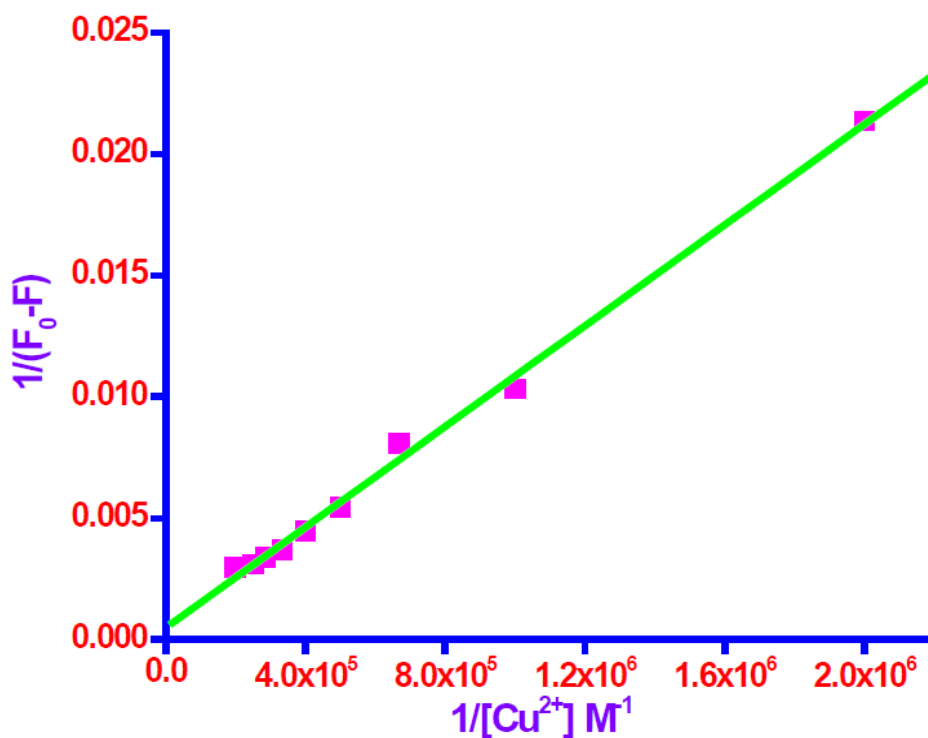


Figure S31. Benesi-Hildebrand plot $I / (F_0 - F)$ vs. $1/[Cu^{2+}]$ for complexation between **5h** and Cu^{2+} derived from emission titration curve.

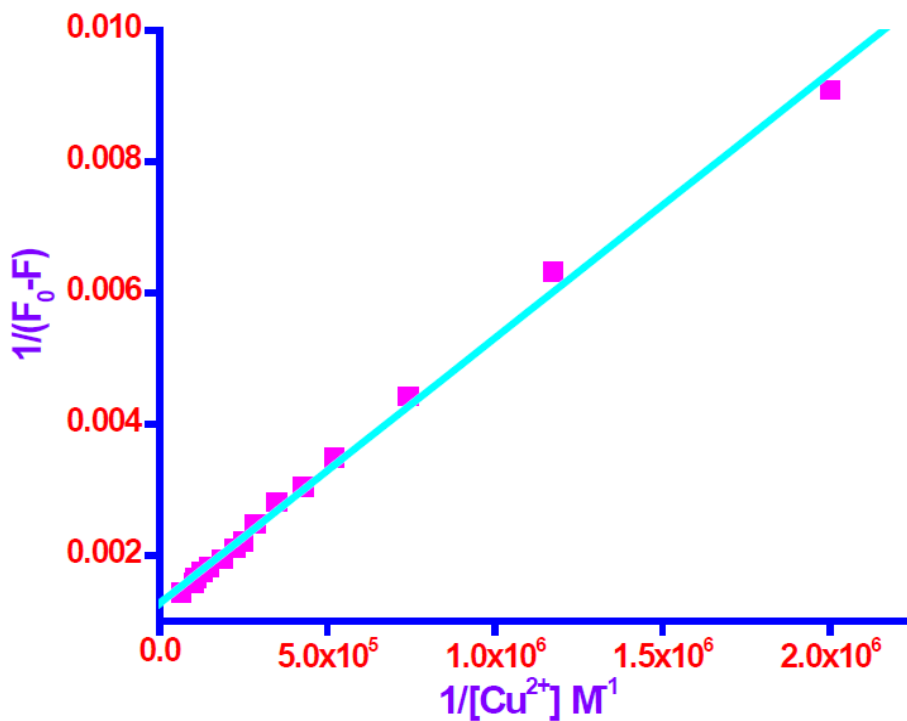


Figure S32. Benesi-Hildebrand plot $I / (F_0 - F)$ vs. $1/[Cu^{2+}]$ for complexation between **5j** and Cu^{2+} derived from emission titration curve.

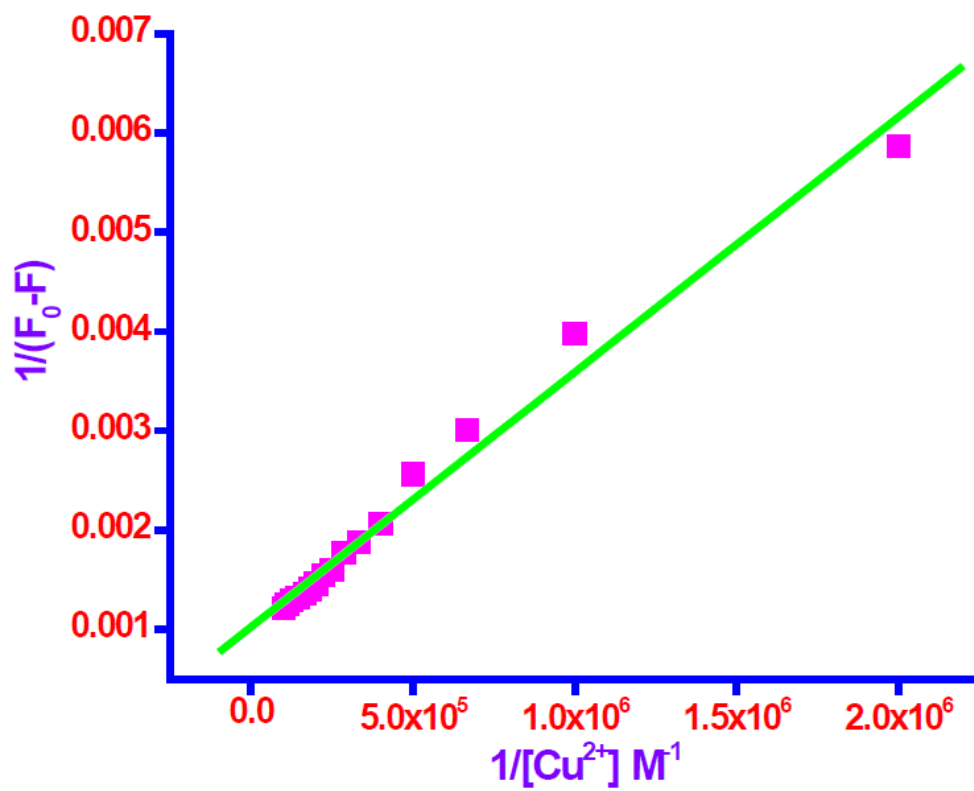


Figure S33. Benesi-Hildebrand plot $1 / (F_0 - F)$ vs. $1/[Cu^{2+}]$ for complexation between **5k** and Cu^{2+} derived from emission titration curve.

Detection limit calculation in emission spectroscopy:

The limit of detection (LOD) of compounds (**5d**, **5f**, **5h**, **5j**, **5k**) with Cu^{2+} was measured on the basis of fluorescence titration measurement. The detection limit was calculated using the following equation:

$$DL = K \times \frac{\sigma}{S}$$

where $K = 2$ or 3 (we take 3 in this case), ' σ ' is the standard deviation of the blank solution and ' S ' is the slope between the ratio of emission intensity *versus* $[\text{Cu}^{2+}]$.

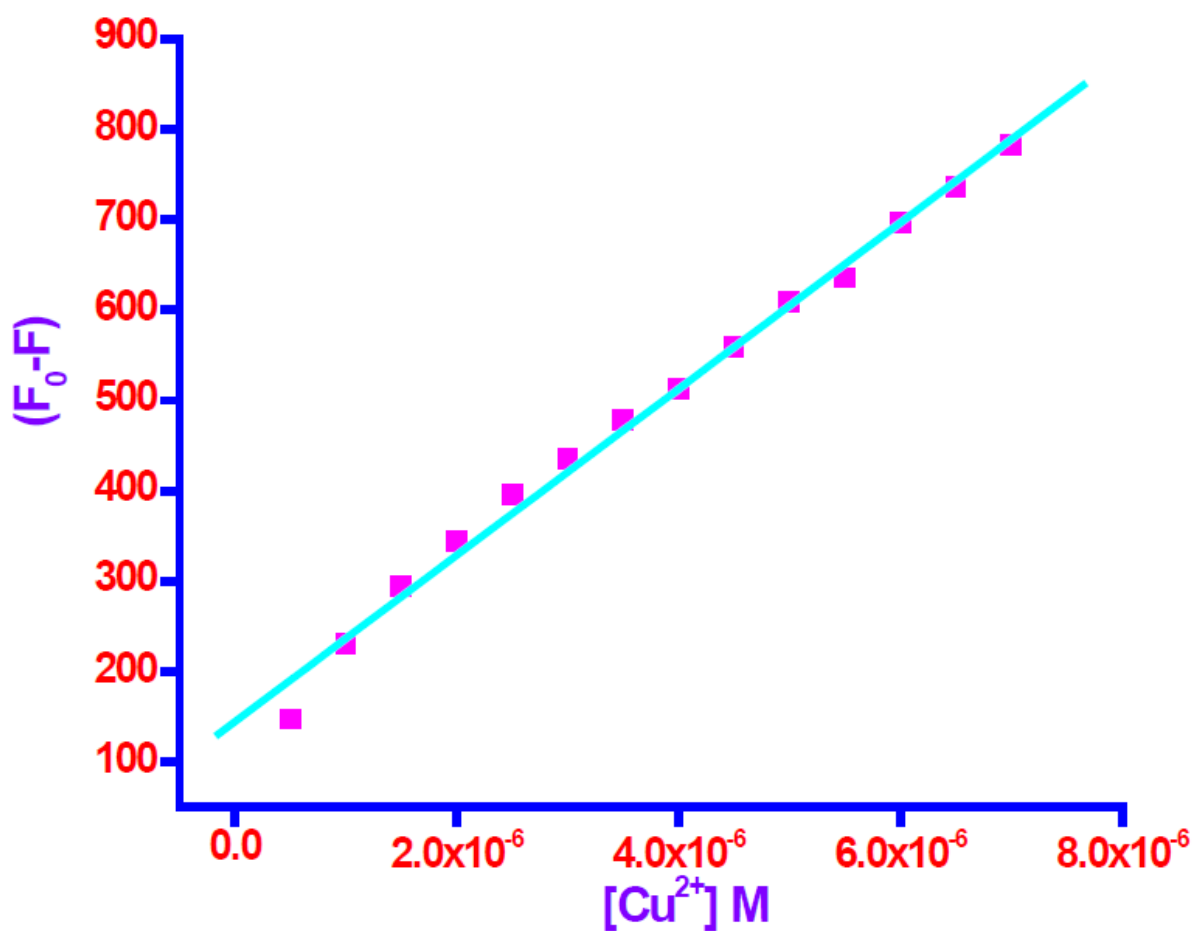


Figure S34. The limit of detection (LOD) of **5d** for Cu^{2+} as a function of $[\text{Cu}^{2+}]$.

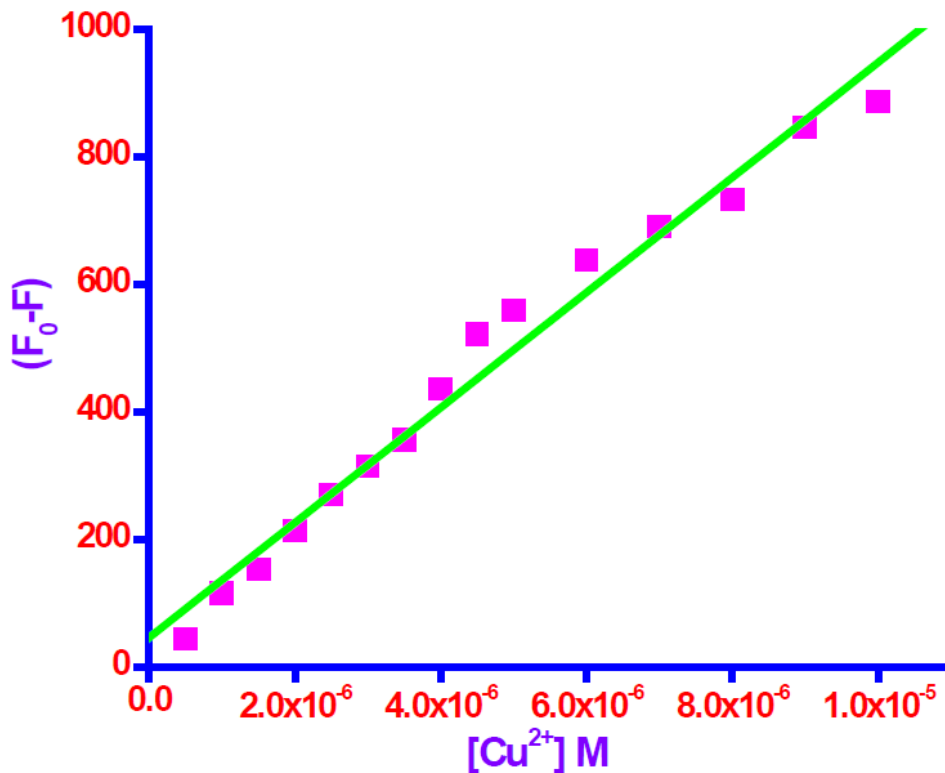


Figure S35. The limit of detection (LOD) of **5f** for Cu²⁺ as a function of [Cu²⁺].

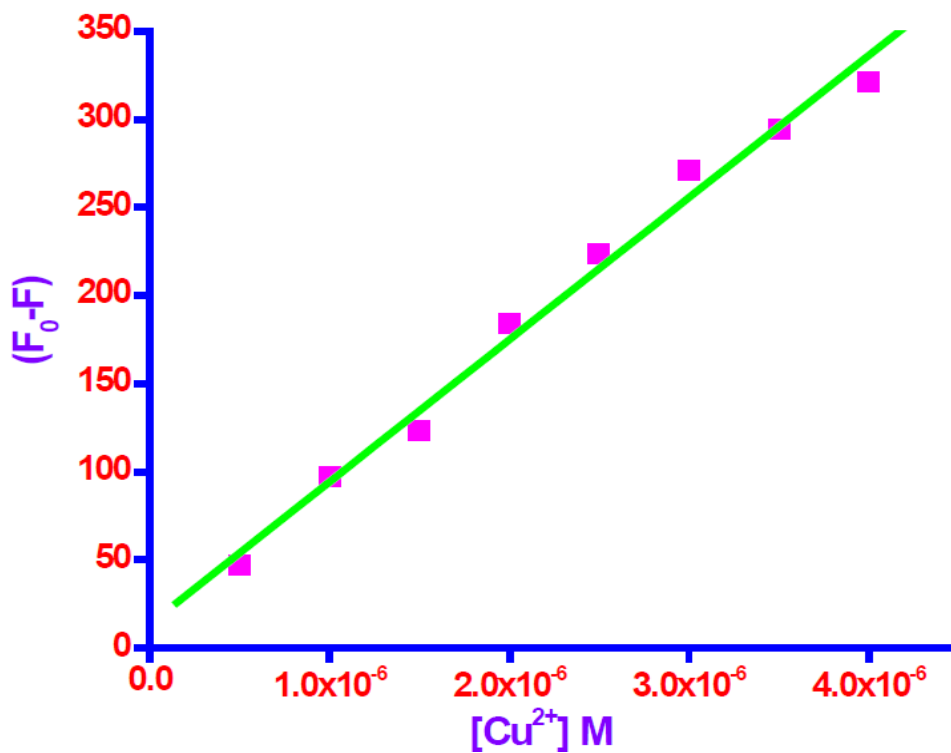


Figure S36. The limit of detection (LOD) of **5h** for Cu²⁺ as a function of [Cu²⁺].

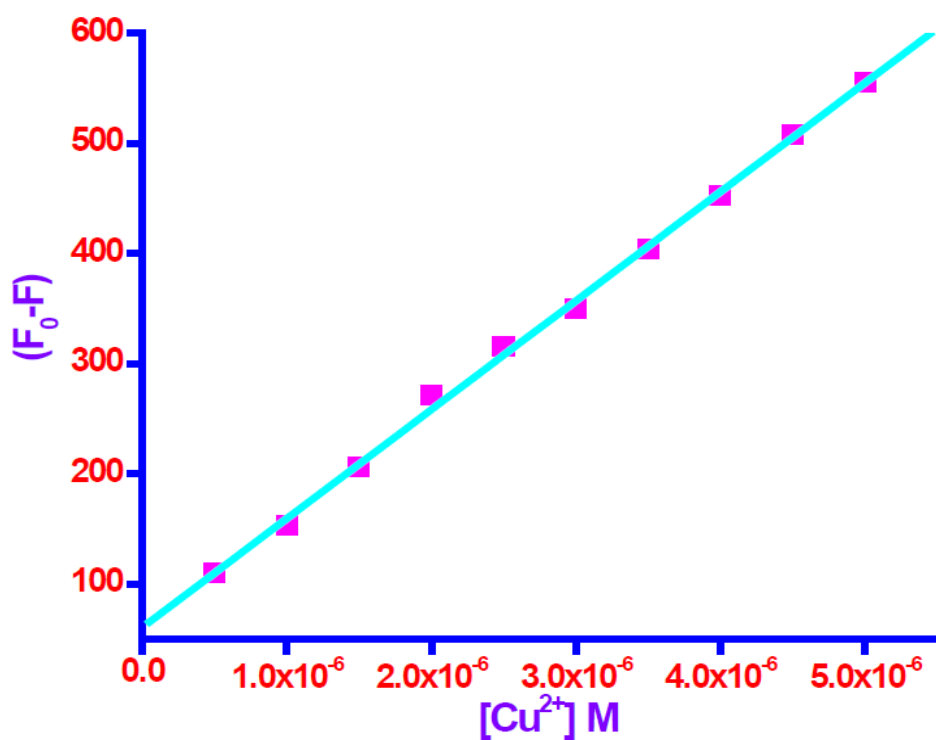


Figure S37. The limit of detection (LOD) of **5j** for Cu²⁺ as a function of [Cu²⁺].

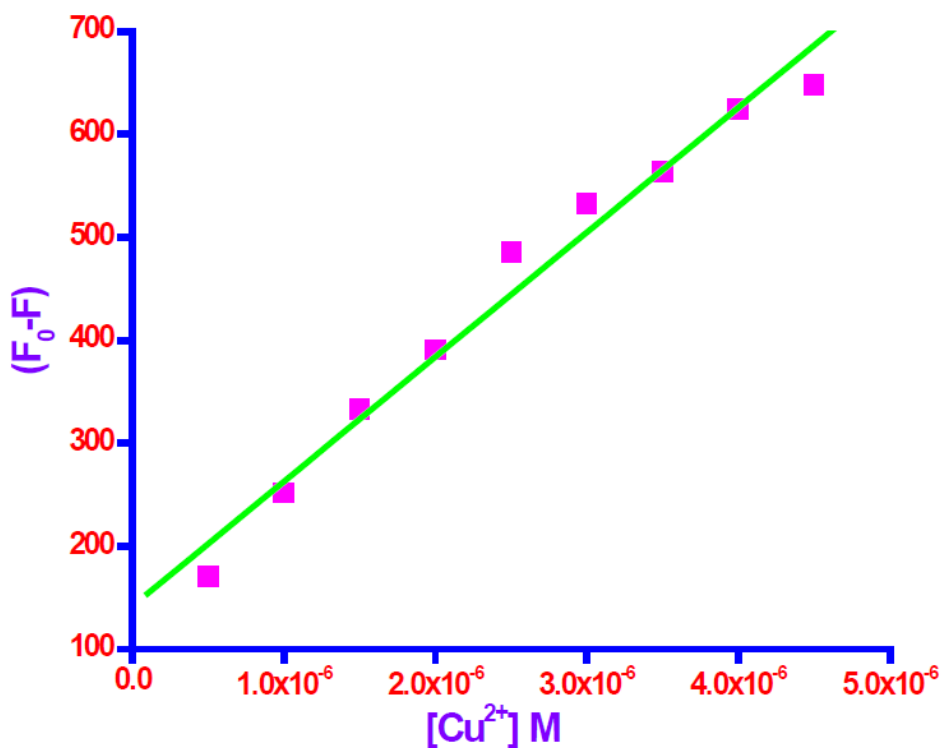


Figure S38. The limit of detection (LOD) of **5k** for Cu²⁺ as a function of [Cu²⁺].

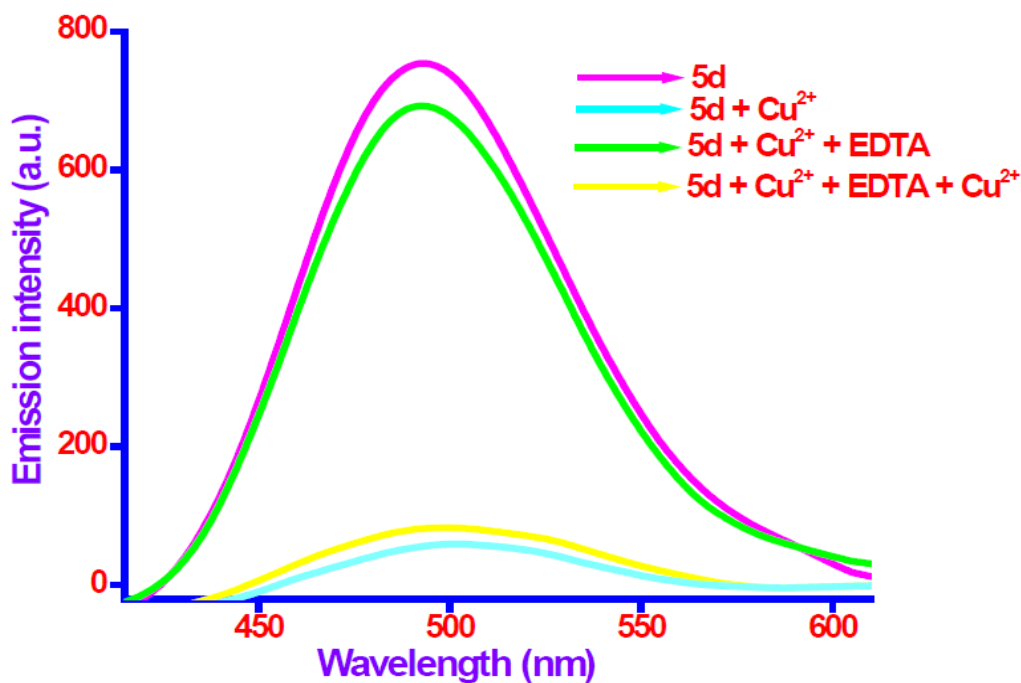


Figure S39. Fluorescence emission spectra of chemosensor (**5d**) in the presence of Cu²⁺ ion followed by addition of EDTA.

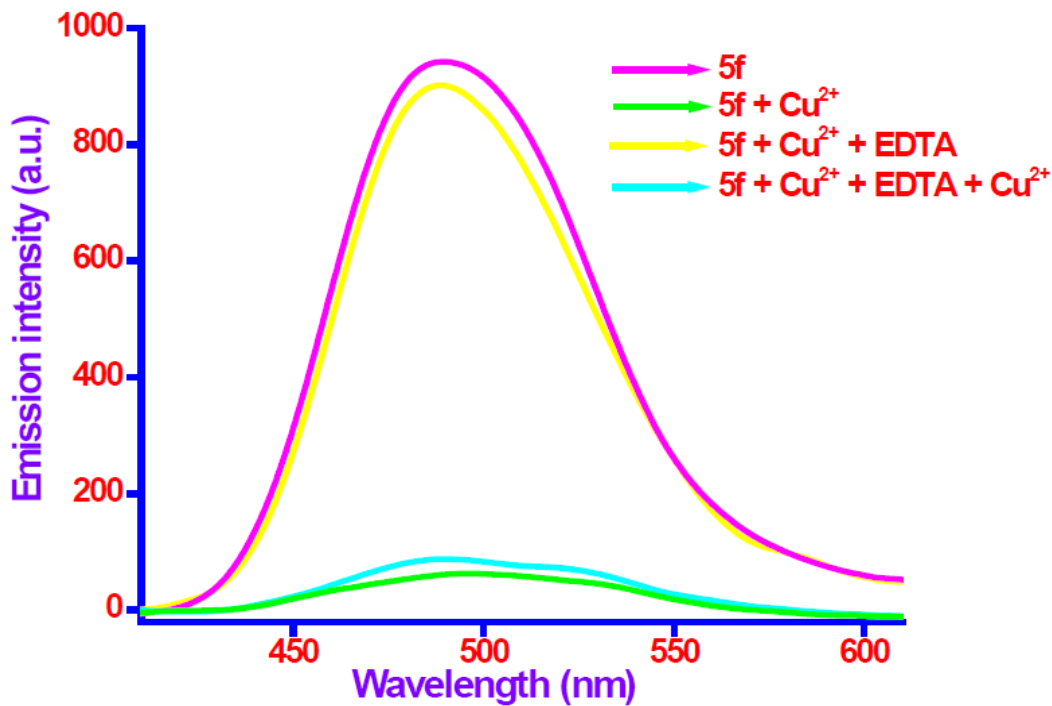


Figure S40. Fluorescence emission spectra of chemosensor (**5f**) in the presence of Cu²⁺ ion followed by addition of EDTA.

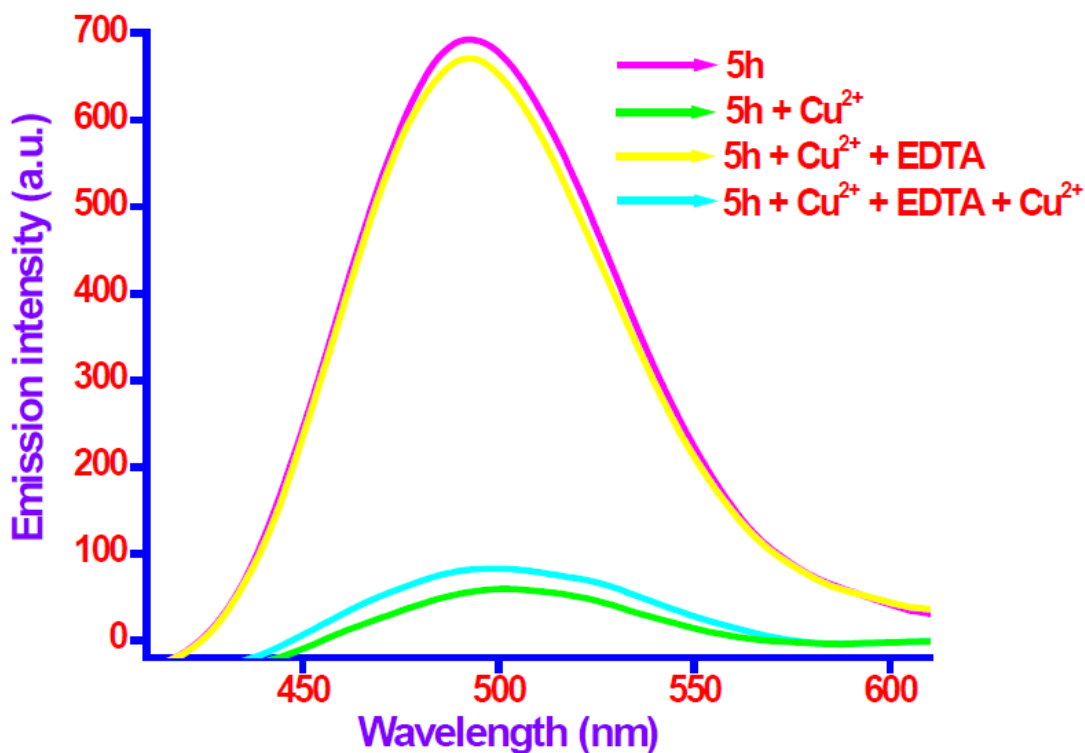


Figure S41. Fluorescence emission spectra of chemosensor (**5h**) in the presence of Cu²⁺ ion followed by addition of EDTA.

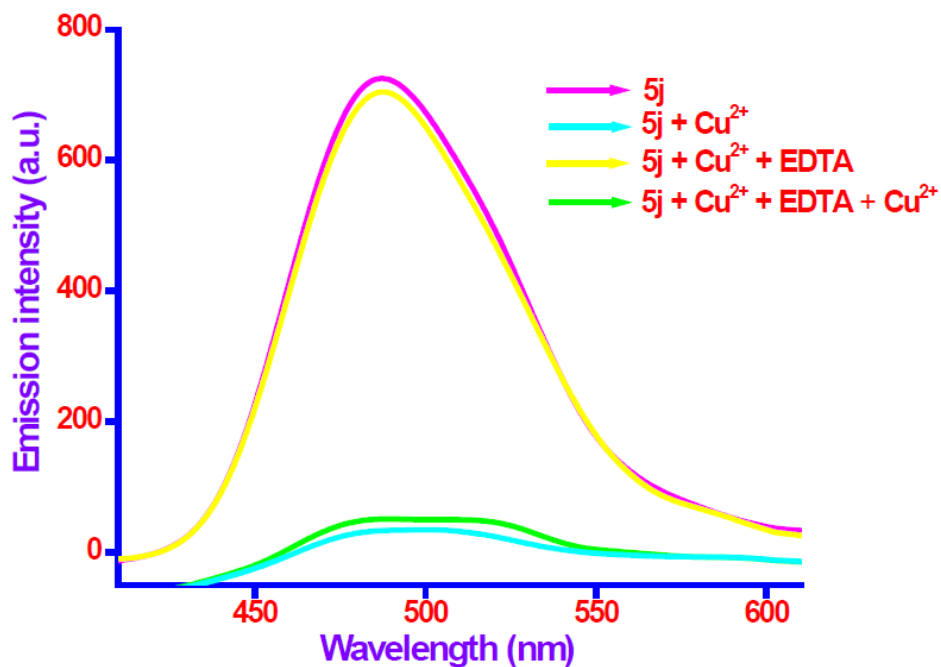


Figure S42. Fluorescence emission spectra of chemosensor (**5j**) in the presence of Cu²⁺ ion followed by addition of EDTA.

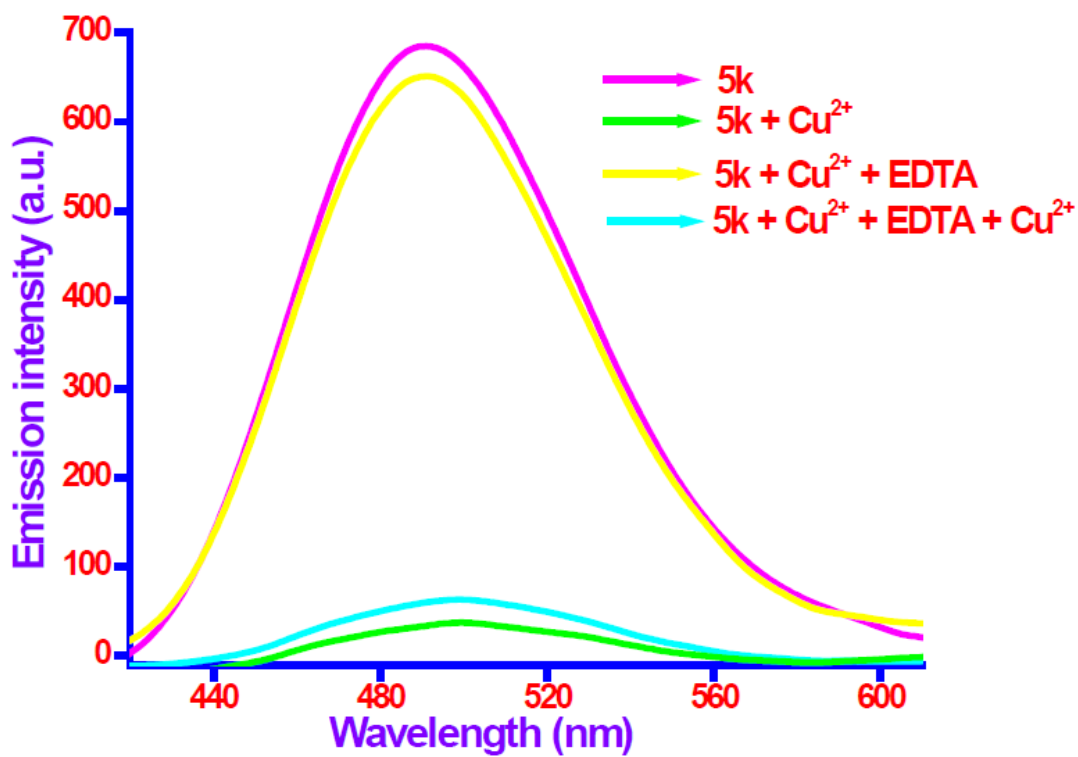


Figure S43. Fluorescence emission spectra of chemosensor (**5k**) in the presence of Cu²⁺ ion followed by addition of EDTA.

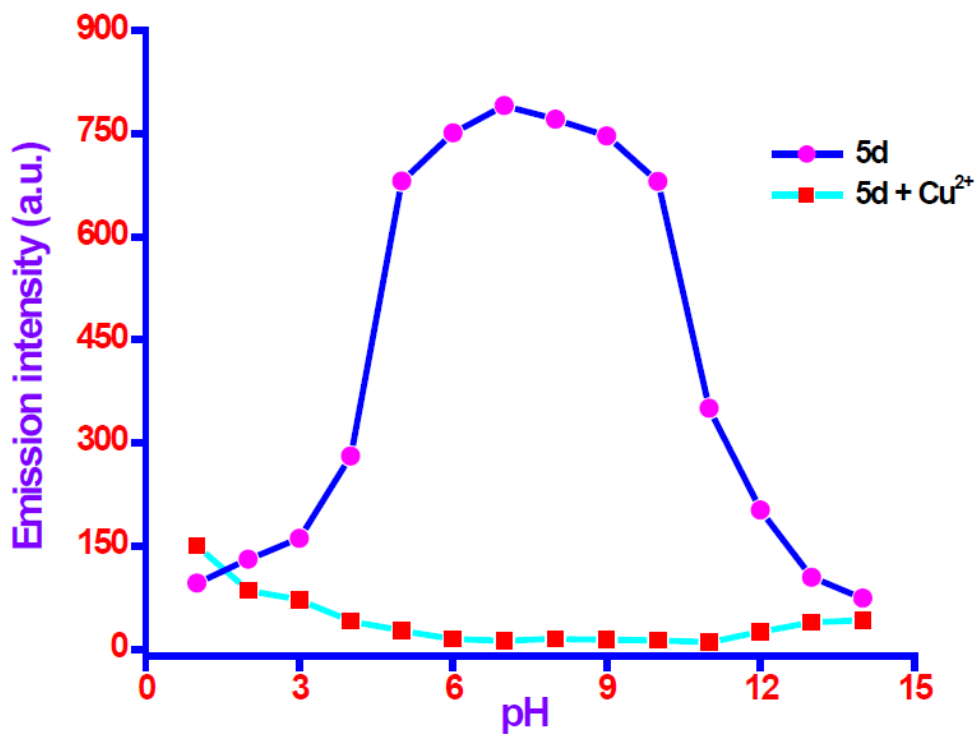


Figure S44. Emission intensity of **5d** (5×10^{-6} M) in absence and in presence of Cu^{2+} as a function of pH values in aqueous DMSO solution at 493.5 nm.

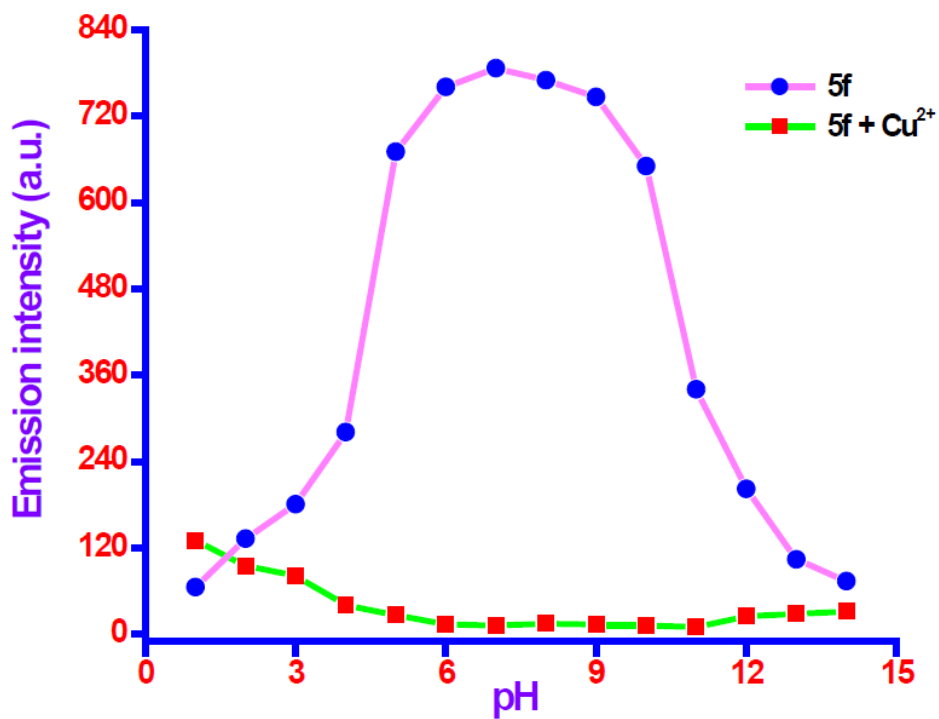


Figure S45. Emission intensity of **5f** (5×10^{-6} M) in absence and in presence of Cu^{2+} as a function of pH values in aqueous DMSO solution at 491.7 nm.

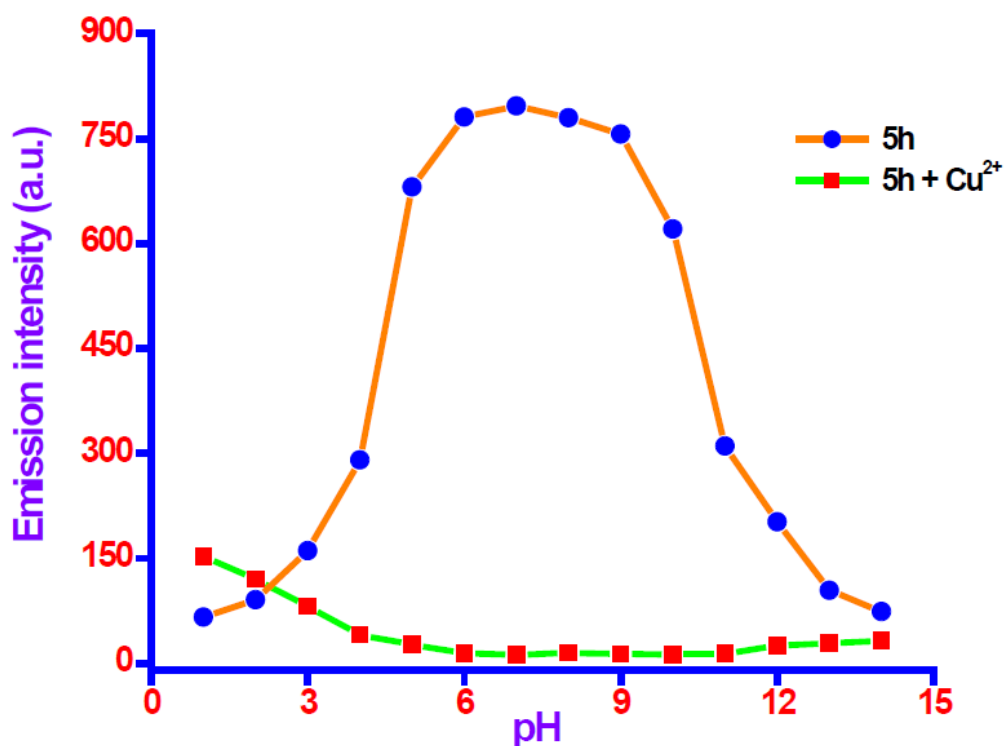


Figure S46. Emission intensity of **5h** (5×10^{-6} M) in absence and in presence of Cu^{2+} as a function of pH values in aqueous DMSO solution at 498.7 nm.

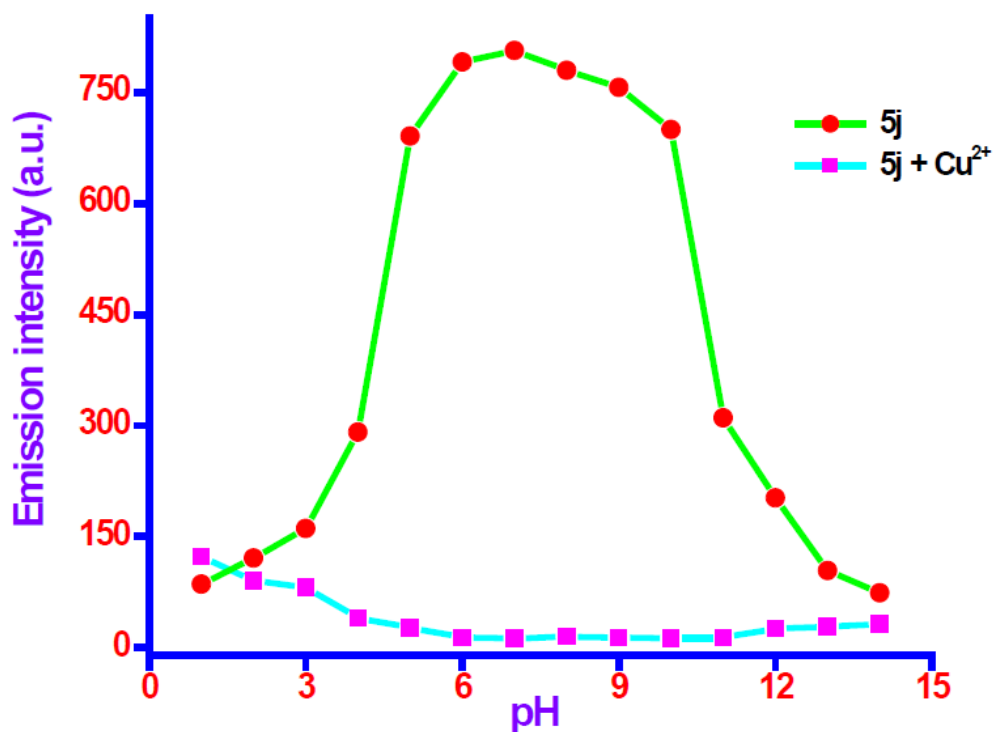


Figure S47. Emission intensity of **5j** (5×10^{-6} M) in absence and in presence of Cu^{2+} as a function of pH values in aqueous DMSO solution at 497.8 nm.

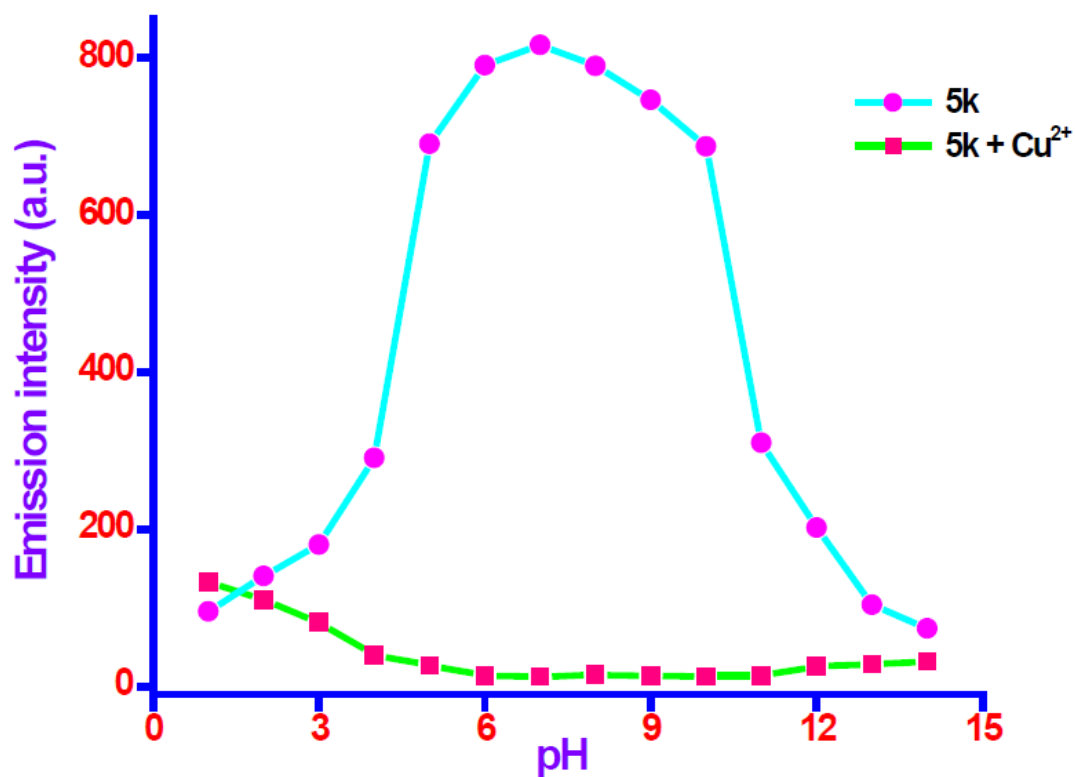


Figure S48. Emission intensity of **5k** (5×10^{-6} M) in absence and in presence of Cu^{2+} as a function of pH values in aqueous DMSO solution at 503.5 nm.